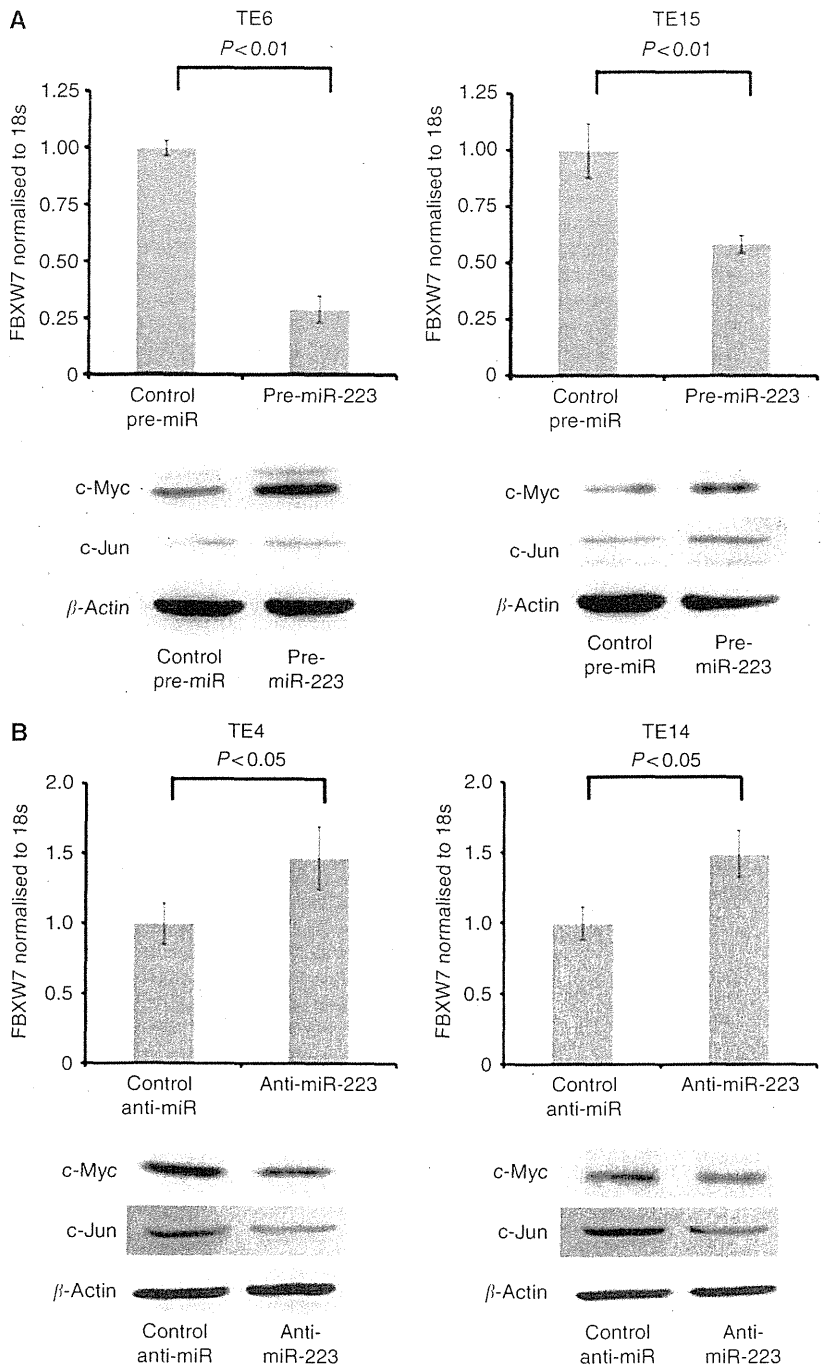

Figure 4 miR-223 gain-of-function and loss-of-function studies in ESCC cell lines. (**A**) The expression of the FBXW7 mRNA was significantly suppressed by transfection of cells with pre-miR-223, as confirmed by qRT–PCR in TE6 and TE15 cells. Furthermore, the expression of the c-Myc and c-Jun proteins was enhanced by treatment with pre-miR-223 as determined by a western blotting analysis. (**B**) In contrast, the FBXW7 mRNA level was significantly increased by transfection of TE4 and TE14 cells with anti-miR-223, and the c-Myc and c-Jun proteins were deregulated.

samples from ESCC patients. When the FBXW7 protein was expressed at high levels, the expression levels of the c-Myc and c-Jun proteins were below the limits of detection in the miR-223 low expression cases (Figures 3A–C). In contrast, in cases with low FBXW7 protein expression, a strong expression of the c-Myc and c-Jun proteins was noted in the cases with high miR-223 expression (Figures 3D–F).

There is an inverse correlation between miR-223 and *FBXW7 in vitro*

Across all the eight cell lines tested, there was a significant inverse correlation between the expression levels of miR-223 and *FBXW7* mRNA (Pearson correlation, $r = -0.855$; $P = 0.007$; Supplementary Figure 2). TE6 and TE15 cells were used to evaluate the effects of

the upregulation of miR-223, and TE4 and TE14 cells were used to examine how the downregulation of miR-223 affected the *FBXW7* expression. *FBXW7* mRNA significantly decreased when cells were transfected with pre-miR-223, compared with those transfected with the negative control (Figure 4A).

Furthermore, we found that the protein expression levels of c-Myc and c-Jun were enhanced after pre-miR-223 treatment by a western blot analysis. In contrast, the TE4 and TE14 cells transfected with anti-miR-223 showed a decrease in the miR-223 expression, compared with the negative control-treated cells. The *FBXW7* mRNA level was significantly increased in the cells transfected with anti-miR-223, compared with those transfected with the negative control, and the protein expression levels of c-Myc and c-Jun were deregulated in these cells (Figure 4B).

DISCUSSION

In our present study, we found that miR-223 was significantly overexpressed in human ESCC tissue compared with the corresponding normal tissue ($P<0.001$), and that the patients with a high miR-223 expression had a significantly poorer prognosis than those with a low expression ($P=0.034$). We also provide evidence that a negative association exists between the expression of miR-223 and the FBXW7 protein in ESCC patients (Pearson correlation, $r=-0.336$; $P<0.01$), and revealed that the miR-223 expression responds to alterations in the c-Myc and c-Jun protein levels as regulated by the FBXW7 pathway *in vitro*. These findings suggested that the overexpression of miR-223 correlates with the poor prognosis of ESCC, possibly because of repression of the function of the FBXW7 protein.

Loss of FBXW7 function is known to be associated with the dysregulation of several cell cycle regulators, including cyclin E and c-Myc (Welcker *et al*, 2003). In oesophagaeal cancer, amplification and overexpression of these regulators has been thoroughly investigated, and their clinical significance has been reported. Cyclin E, a maintainer of the cell cycle restriction point, is significantly overexpressed in mucosal invasive ESCC compared with normal mucosa (Ohbu *et al*, 2001). The amplification of c-Myc was more frequently found in advanced stages of ESCC than in early stages (Bitzer *et al*, 2003). Therefore, the regulation of FBXW7 may have an important role in the carcinogenesis and progression of ESCC. In this study, there was an inverse correlation between FBXW7, and c-Myc and c-Jun in ESCC samples as indicated by an immunohistochemical analysis. Moreover, an *in vitro* assay demonstrated that there was a decrease in the *FBXW7* expression when miR-223 was overexpressed, which gave rise to an abnormal accumulation of the c-Myc and c-Jun proteins.

miR-223 has been recently reported to have a potential role in tumourigenesis through repressing the function of FBXW7, and the overexpression of miR-223 has been shown to significantly reduce the *FBXW7* mRNA levels, while increasing both the endogenous cyclin E protein and activity levels, as well as genomic instability (Xu *et al*, 2010). Moreover, a recent report identified miR-223 as an E2F1 transcriptional target (Pulikkan *et al*, 2010), and E2F1 and miR-223 comprised an autologous negative feedback loop. These facts indicate that miR-223 is one of the key players in cell cycle regulation at the G1–S transition. In addition, miR-223 has been reported to act as an oncogene in several solid tumours, including gastric, ovarian, and bladder cancers (Gottardo *et al*, 2007; Laios *et al*, 2008; Petrocca *et al*, 2008). Moreover, in gastric cancer, the expression level of miR-223 was reported to be a prognostic marker (Li *et al*, 2010). On the other hand, there has been another report suggesting that miR-223 acts as a tumour suppressor by directly targeting Stathmin1 to stimulate the development and progression of hepatocellular carcinoma (Wong *et al*, 2008). In addition, Li *et al* (2011) revealed the oncogene Artemin to be a target of miR-223 and the overexpression of miR-223 decreased the migration and invasion of oesophageal carcinoma cells. Therefore, on the basis of their findings, miR-223 may have a tumour-suppressor function in oesophageal carcinoma. However, in the current study, on the basis of an investigation of 109 ESCC clinical samples, we showed that miR-223 was significantly overexpressed in the tumour compared with the corresponding normal tissue. We also found that the overexpression of miR-223 correlated with tumour advancement and a poor prognosis. Moreover, in a series of gain-of-function and loss-of-function investigations, we found that these effects may be due to the downregulation of the tumour-suppressor FBXW7, which was targeted by miR-223. The decrease in the expression of *FBXW7* resulting from the overexpression of miR-223 gave rise to the abnormal accumulation of c-Myc and c-Jun proteins. It is well known that one miRNA can regulate many targets and, therefore, it may be possible that the same miRNA may have opposite roles in the progression of cancer in different tissues (Shenouda and Alahari, 2009). As miR-223 also targets other genes, some are oncogenes whereas others are tumour-suppressor genes, further analyses are needed to elucidate the full spectrum of miR-223 functions.

Although we suggested that miR-223 regulates FBXW7, 16 out of 74 samples with high miR-223 expression still showed FBXW7 expression and 12 out of 35 samples with low miR-223 expression did not show FBXW7 as shown in Table 1. The relationship between miR-223 and FBXW7 was therefore not completely inverse. To explain this finding, we speculate that not only miR-223 but also various other mechanisms, have effects on the expression of FBXW7, such as epigenetic transcriptional regulation (Gu *et al*, 2008), the loss of genetic alteration (Iwatsuki *et al*, 2010), the status of *p53* mutation (Yokobori *et al*, 2009), or the regulation by other miRs (miR-25, 27a, 92a) (Xu *et al*, 2010).

In conclusion, the present study at first indicates that a high expression level of miR-223 had a significant adverse impact on the survival of ESCC patients through repression of the function of FBXW7.

ACKNOWLEDGEMENTS

This work was supported in part by the following grants and foundations: Japan Society for the Promotion of Science (JSPS) Grant-in-Aid for Scientific Research; grant numbers 23791550, Takeda Science Foundation 2010, Okukubo Memorial Fund for Medical Research in Kumamoto University School of Medicine 2010, Uehara Memorial Foundation 2010, YOKOYAMA Foundation for Clinical Pharmacology 2011.

Supplementary Information accompanies the paper on British Journal of Cancer website (http://www.nature.com/bjc)

REFERENCES

Ambros V (2004) The functions of animal microRNAs. *Nature* **431**(7006): 350–355

Bitzer M, Stahl M, Arjumand J, Rees M, Klump B, Heep H, Gabbert HE, Sarbia M (2003) C-myc gene amplification in different stages of oesophageal squamous cell carcinoma: prognostic value in relation to treatment modality. *Anticancer Res* **23**(2B): 1489–1493

Bloomston M, Frankel WL, Petrocca F, Volinia S, Alder H, Hagan JP, Liu CG, Bhatt D, Taccioli C, Croce CM (2007) MicroRNA expression

patterns to differentiate pancreatic adenocarcinoma from normal pancreas and chronic pancreatitis. *JAMA* **297**(17): 1901–1908

Bredel M, Bredel C, Juric D, Harsh GR, Vogel H, Recht LD, Sikic BI (2005) Functional network analysis reveals extended gliomagenesis pathway maps and three novel MYC-interacting genes in human gliomas. *Cancer Res* **65**(19): 8679–8689

Calin GA, Liu CG, Sevignani C, Ferracin M, Felli N, Dumitru CD, Shimizu M, Cimmino A, Zupo S, Dono M, Dell'Aquila ML, Alder H, Rassenti L, Kipps TJ, Bullrich F, Negrini M, Croce CM (2004) MicroRNA profiling reveals distinct signatures in B cell chronic lymphocytic leukemias. *Proc Natl Acad Sci USA* **101**(32): 11755–11760

Croce CM, Calin GA (2005) miRNAs, cancer, and stem cell division. *Cell* **122**(1): 6–7

Gottardo F, Liu CG, Ferracin M, Calin GA, Fassan M, Bassi P, Sevignani C, Byrne D, Negrini M, Pagano F, Gomella LG, Croce CM, Baffa R (2007) Micro-RNA profiling in kidney and bladder cancers. *Urol Oncol* **25**(5): 387–392

Gu Z, Mitsui H, Inomata K, Honda M, Endo C, Sakurada A, Sato M, Okada Y, Kondo T, Horii A (2008) The methylation status of FBXW7 beta-form correlates with histological subtype in human thymoma. *Biochem Biophys Res Commun* **377**(2): 685–688

Hagedorn M, Delugin M, Abraldes I, Allain N, Belaud-Rotureau MA, Turmo M, Prigent C, Loiseau H, Bikfalvi A, Javerzat S (2007) FBXW7/hCDC4 controls glioma cell proliferation *in vitro* and is a prognostic marker for survival in glioblastoma patients. *Cell Div* **2**: 9

Hiyoshi Y, Kamohara H, Karashima R, Sato N, Imamura Y, Nagai Y, Yoshida N, Toyama E, Hayashi N, Watanabe M, Baba H (2009) MicroRNA-21 regulates the proliferation and invasion in esophageal squamous cell carcinoma. *Clin Cancer Res* **15**(6): 1915–1922

Ibusuki M, Yamamoto Y, Shinriki S, Ando Y, Iwase H (2011) Reduced expression of ubiquitin ligase FBXW7 mRNA is associated with poor prognosis in breast cancer patients. *Cancer Sci* **102**(2): 439–445

Inuzuka H, Shaik S, Onoyama I, Gao D, Tseng A, Maser RS, Zhai B, Wan L, Gutierrez A, Lau AW, Xiao Y, Christie AL, Aster J, Settleman J, Gygi SP, Kung AL, Look T, Nakayama KI, DePinho RA, Wei W (2011) SCF(FBW7) regulates cellular apoptosis by targeting MCL1 for ubiquitylation and destruction. *Nature* **471**(7336): 104–109

Iwatsuki M, Mimori K, Ishii H, Yokobori T, Takatsuno Y, Sato T, Toh H, Onoyama I, Nakayama KI, Baba H, Mori M (2010) Loss of FBXW7, a cell cycle regulating gene, in colorectal cancer: clinical significance. *Int J Cancer* **126**(8): 1828–1837

Laios A, O'Toole S, Flavin R, Martin C, Kelly L, Ring M, Finn SP, Barrett C, Loda M, Gleeson N, D'Arcy T, McGuinness E, Sheils O, Sheppard B, O'Leary J (2008) Potential role of miR-9 and miR-223 in recurrent ovarian cancer. *Mol Cancer* **7**: 35

Li S, Li Z, Guo F, Qin X, Liu B, Lei Z, Song Z, Sun L, Zhang HT, You J, Zhou Q (2011) miR-223 regulates migration and invasion by targeting Artemin in human esophageal carcinoma. *J Biomed Sci* **18**: 24

Li X, Zhang Y, Ding J, Wu K, Fan D (2010) Survival prediction of gastric cancer by a seven-microRNA signature. *Gut* **59**(5): 579–585

Mao JH, Kim IJ, Wu D, Climent J, Kang HC, DelRosario R, Balmain A (2008) FBXW7 targets mTOR for degradation and cooperates with PTEN in tumor suppression. *Science* **321**(5895): 1499–1502

Meister G (2007) miRNAs get an early start on translational silencing. *Cell* **131**(1): 25–28

Nakayama KI, Nakayama K (2006) Ubiquitin ligases: cell-cycle control and cancer. *Nat Rev Cancer* **6**(5): 369–381

Ohbu M, Kobayashi N, Okayasu I (2001) Expression of cell cycle regulatory proteins in the multistep process of oesophageal carcinogenesis: stepwise over-expression of cyclin E and p53, reduction of p21(WAF1/CIP1) and dysregulation of cyclin D1 and p27(KIP1). *Histopathology* **39**(6): 589–596

Petrocca F, Visone R, Onelli MR, Shah MH, Nicoloso MS, de Martino I, Iliopoulos D, Pilozzi E, Liu CG, Negrini M, Cavazzini L, Volinia S, Alder H, Ruco LP, Baldassarre G, Croce CM, Vecchione A (2008) E2F1-regulated microRNAs impair TGFbeta-dependent cell-cycle arrest and apoptosis in gastric cancer. *Cancer Cell* **13**(3): 272–286

Pulikkan JA, Dengler V, Peramangalam PS, Peer Zada AA, Muller-Tidow C, Bohlander SK, Tenen DG, Behre G (2010) Cell-cycle regulator E2F1 and microRNA-223 comprise an autoregulatory negative feedback loop in acute myeloid leukemia. *Blood* **115**(9): 1768–1778

Schetter AJ, Leung SY, Sohn JJ, Zanetti KA, Bowman ED, Yanaihara N, Yuen ST, Chan TL, Kwong DL, Au GK, Liu CG, Calin GA, Croce CM, Harris CC (2008) MicroRNA expression profiles associated with prognosis and therapeutic outcome in colon adenocarcinoma. *JAMA* **299**(4): 425–436

Shenouda SK, Alahari SK (2009) MicroRNA function in cancer: oncogene or a tumor suppressor? *Cancer Metastasis Rev* **28**(3–4): 369–378

Ueda T, Volinia S, Okumura H, Shimizu M, Taccioli C, Rossi S, Alder H, Liu CG, Oue N, Yasui W, Yoshida K, Sasaki H, Nomura S, Seto Y, Kaminishi M, Calin GA, Croce CM (2010) Relation between microRNA expression and progression and prognosis of gastric cancer: a microRNA expression analysis. *Lancet Oncol* **11**(2): 136–146

Welcker M, Clurman BE (2008) FBW7 ubiquitin ligase: a tumour suppressor at the crossroads of cell division, growth and differentiation. *Nat Rev Cancer* **8**(2): 83–93

Welcker M, Singer J, Loeb KR, Grim J, Bloecher A, Gurien-West M, Clurman BE, Roberts JM (2003) Multisite phosphorylation by Cdk2 and GSK3 controls cyclin E degradation. *Mol Cell* **12**(2): 381–392

Wertz IE, Kusam S, Lam C, Okamoto T, Sandoval W, Anderson DJ, Helgason E, Ernst JA, Eby M, Liu J, Belmont LD, Kaminker JS, O'Rourke KM, Pujara K, Kohli PB, Johnson AR, Chiu ML, Lill JR, Jackson PK, Fairbrother WJ, Seshagiri S, Ludlam MJ, Leong KG, Dueber EC, Maecker H, Huang DC, Dixit VM (2011) Sensitivity to antitubulin chemotherapeutics is regulated by MCL1 and FBW7. *Nature* **471**(7336): 110–114

Wong QW, Lung RW, Law PT, Lai PB, Chan KY, To KF, Wong N (2008) MicroRNA-223 is commonly repressed in hepatocellular carcinoma and potentiates expression of Stathmin1. *Gastroenterology* **135**(1): 257–269

Xu Y, Sengupta T, Kukreja L, Minella AC (2010) MicroRNA-223 regulates cyclin E activity by modulating expression of F-box and WD-40 domain protein 7. *J Biol Chem* **285**(45): 34439–34446

Yanaihara N, Caplen N, Bowman E, Seike M, Kumamoto K, Yi M, Stephens RM, Okamoto A, Yokota J, Tanaka T, Calin GA, Liu CG, Croce CM, Harris CC (2006) Unique microRNA molecular profiles in lung cancer diagnosis and prognosis. *Cancer Cell* **9**(3): 189–198

Yokobori T, Mimori K, Iwatsuki M, Ishii H, Onoyama I, Fukagawa T, Kuwano H, Nakayama KI, Mori M (2009) p53-Altered FBXW7 expression determines poor prognosis in gastric cancer cases. *Cancer Res* **69**(9): 3788–3794

Zamore PD, Haley B (2005) Ribo-gnome: the big world of small RNAs. *Science* **309**(5740): 1519–1524

Thrombospondin-1 Is a Novel Negative Regulator of Liver Regeneration After Partial Hepatectomy Through Transforming Growth Factor-beta1 Activation in Mice

Hiromitsu Hayashi,[1] Keiko Sakai,[1] Hideo Baba,[2] and Takao Sakai[1,3]

The matricellular protein, thrombospondin-1 (TSP-1), is prominently expressed during tissue repair. TSP-1 binds to matrix components, proteases, cytokines, and growth factors and activates intracellular signals through its multiple domains. TSP-1 converts latent transforming growth factor-beta1 (TGF-β1) complexes into their biologically active form. TGF-β plays significant roles in cell-cycle regulation, modulation of differentiation, and induction of apoptosis. Although TGF-β1 is a major inhibitor of proliferation in cultured hepatocytes, the functional requirement of TGF-β1 during liver regeneration remains to be defined *in vivo*. We generated a TSP-1-deficient mouse model of a partial hepatectomy (PH) and explored TSP-1 induction, progression of liver regeneration, and TGF-β-mediated signaling during the repair process after hepatectomy. We show here that TSP-1-mediated TGF-β1 activation plays an important role in suppressing hepatocyte proliferation. TSP-1 expression was induced in endothelial cells (ECs) as an immediate early gene in response to PH. TSP-1 deficiency resulted in significantly reduced TGF-β/Smad signaling and accelerated hepatocyte proliferation through down-regulation of p21 protein expression. TSP-1 induced in ECs by reactive oxygen species (ROS) modulated TGF-β/Smad signaling and proliferation in hepatocytes *in vitro*, suggesting that the immediately and transiently produced ROS in the regenerating liver were the responsible factor for TSP-1 induction. *Conclusions:* We have identified TSP-1 as an inhibitory element in regulating liver regeneration by TGF-β1 activation. Our work defines TSP-1 as a novel immediate early gene that could be a potential therapeutic target to accelerate liver regeneration. (HEPATOLOGY 2012;55:1562-1573)

Cell proliferation is part of the wound-healing response and plays a central role in regeneration after tissue damage. It is crucial to advance our understanding of the molecular mechanisms underlying tissue regeneration and to develop a novel strategy to enhance the regenerative process. Such knowledge, in turn, would yield clinical benefits, such as decreased morbidity and mortality. Partial hepatectomy (PH) is a well-established model system in rodents for studying the molecular mechanisms of liver regeneration. PH triggers activation of the immediate early genes (i.e., genes that are rapidly, but transiently, activated) within approximately the first 4 hours,[1] and thereby hepatocytes reenter the cell-division cycle. Immediate early genes encode proteins that regulate later phases in G_1 and play an important role in cell growth in the regenerating liver.[1,2] The process of liver regeneration after hepatectomy is coordinated by both pro- and antiproliferative factors. Transforming growth factor-beta1 (TGF-β1) is a potent inhibitor of mitogen-stimulated DNA synthesis in cultured hepatocytes.[3] Therefore, it has been thought that TGF-β1 is a potent candidate to

Abbreviations: BrdU, 5-bromo-2-deoxyuridine; CD, cluster of differentiation; CM, conditioned media; ECs, endothelial cells; Erk1/2, extracellular signal-related kinase 1 and 2; HSC, hepatic stellate cell; HUVEC, human umbilical vein endothelial cell; ICC, immunocytochemistry; IF, immunofluorescence; IHC, immunohistochemical; MDA, malondialdehyde; mRNA, messenger RNA; NAC, N-acetylcysteine; PAI-1, plasminogen activator inhibitor-1; PECAM-1, platelet/endothelial cell adhesion molecule-1; PCR, polymerase chain reaction; PH, partial hepatectomy; PI3K, phosphatidylinositide 3-kinase; (PI3K ROS, reactive oxygen species; α-SMA, alpha smooth muscle actin; STAT3, signal transducer and activator of transcription 3; TSP-1, thrombospondin-1; TGF-β1, transforming growth factor-β1; TUNEL, terminal deoxynucleotidyl transferase dUTP nick end labeling; VEGFR, vascular endothelial growth factor-A receptor; WT, wild type.

From the [1]Department of Biomedical Engineering, Lerner Research Institute, Cleveland Clinic, Cleveland, OH; [2]Department of Gastroenterological Surgery, Graduate School of Medical Sciences, Kumamoto University, Kumamoto, Japan; and [3]Orthopedic and Rheumatologic Research Center, Cleveland Clinic, Cleveland, OH.

Received August 12, 2011; accepted November 1, 2011.

This work was supported by the National Institutes of Health (grant no.: R01 DK074538; to T.S.) and the Byotai Taisha Research Foundation and Uehara Memorial Foundation, Japan (to H.H.).

limit or stop liver regeneration after PH.[4] Because TGF-β is synthesized and secreted as a latent complex, the important step in regulating its biological activity is the conversion of the latent form into the active one. However, the contribution of TGF-β to the liver's regenerative response after PH is still poorly understood. *TGF-β1* messenger RNA (mRNA) induction occurs within 4 hours, and levels of TGF-β1 remain elevated until 72 hours after PH.[5,6] In sharp contrast, in the model of complete lack of TGF-β signaling using hepatocyte-specific *TGF-β type II receptor* knockout mice, the lack of TGF-β signaling does not result in prolonged hepatocyte proliferation; rather, only transiently up-regulated proliferation of hepatocytes is shown in the later phase after hepatectomy, with a peak at ~36 hours.[7] These differences raise an open question about whether locally activated TGF-β1 is indeed essential for the inhibition of hepatocyte proliferation *in vivo*. Furthermore, the time course of locally activated TGF-β1 and its activation mechanism after PH still remain largely unknown.

The matricellular protein, thrombospondin-1 (TSP-1), was first shown as a component of the α-granule in platelets and can act as a major activator of latent TGF-β1.[8,9] TSP-1 is induced in response to tissue damage or stress and plays a role as a transient component of extracellular matrix during tissue repair.[8,10,11] However, the roles of TSP-1 and of TSP-1/TGF-β1 interdependence during liver regeneration have not yet been addressed. We hypothesize that the initiation of local TGF-β activation occurs much earlier after PH, and TSP-1 plays a critical role in this process. Here, using a TSP-1-deficient mouse model, we investigated whether TSP-1 would be a suitable molecular target for accelerating liver regeneration after PH.

Materials and Methods

Mutant Mice and Animal Studies. TSP-1-null mice were kindly provided by Dr. Jack Lawler (Beth Israel Deaconess Medical Center, Boston, MA).[12] Male wild-type (WT) and TSP-1-null mice, at 8-12 weeks old (C57BL/6 background), were used for the experiments. The two anterior lobes (i.e., median and left lateral lobes), which comprise 70% of liver weight, were resected, whereas the caudate and right lobes were left intact. This study was approved by the institutional animal care and use committee.

Immunostaining and Western Blotting. For histological analyses, liver samples (the same lobe from each mouse) were either directly frozen in OCT compound (Tissue-Tek; Sakura Finetek, Tokyo, Japan) or fixed overnight in 4% paraformaldehyde in phosphate-buffered saline (pH 7.2) and dehydrated in a graded alcohol series and embedded in paraffin. Then, the materials were sectioned at a thickness of 5 μm. Immunofluorescence (IF) and immunohistochemical (IHC) staining was performed as described previously.[13] The negative control staining was performed without the addition of primary antibody. Immunostained slides were viewed under a Leica DM 5500B microscopic system (Leica Microsystems, Buffalo Grove, IL). A minimum of 10 different images were randomly selected, and the data shown are representative of the results observed. Western blotting analysis was performed as described previously.[13] The same lobe from each mouse was used for protein isolation and subsequent analysis. ImageJ software (version 1.40) was used for densitometric analysis.

Assessment of 5-Bromo-2-Deoxyuridine Incorporation. Mice received an intraperitoneal injection of 5-bromo-2-deoxyuridine (BrdU; 100 mg/kg; Roche Applied Science, Indianapolis, IN) 2 hours before sacrifice. Six random visual high-power fields (0.64 mm^2 per field) per mouse were evaluated to determine the number of BrdU-positive nuclei in hepatocytes and nonparenchymal cells. Nonparenchymal cells were defined as cells with smaller, irregularly shaped nuclei, compared with larger, circular nuclei of hepatocytes, as previously described.[14] All BrdU-positive cells, from both cell types, were summed at each time point.

Assessment of Apoptotic Index. Terminal deoxynucleotidyl transferase dUTP nick end labeling (TUNEL) analysis was performed using an *in situ* apoptosis detection kit (Roche). Six visual high-power fields (0.64 mm^2 per field) per mouse were evaluated to determine the number of TUNEL-positive nuclei.

Antibodies. The antibodies used for analyses are summarized in Supporting Table 1. The amount of active and total TGF-β1 in liver samples was determined using an enzyme-linked immunosorbent assay kit (Quantikine

Address reprint requests to: Takao Sakai, M.D., Ph.D., Department of Biomedical Engineering/ND20, Lerner Research Institute, Cleveland Clinic, 9500 Euclid Avenue, Cleveland, OH 44195. E-mail: sakait@ccf.org; fax: +01-216-444-9198.

View this article online at wileyonlinelibrary.com.

DOI 10.1002/hep.24800

Potential conflict of interest: Nothing to report.

Additional Supporting Information may be found in the online version of this article.

TGF-β1 Immunoassay; R&D Systems, Inc., Minneapolis, MN), according to the manufacturer's instructions.

Real-time Polymerase Chain Reaction. Real-time polymerase chain reaction (PCR) was performed as described previously.[13] The primers used are summarized in Supporting Table 2.

Lipid Peroxidation Assay. Liver tissue content of malondialdehyde (MDA) was measured by the thiobarbituric acid reduction method using a commercially available kit (#10009055; Cayman Chemical, Ann Arbor, MI). Values were obtained after 30-minute incubation at 90°C under acidic conditions.

In Vitro Assay Using Human Umbilical Vein Endothelial Cells and Mouse Primary Hepatocytes. Human umbilical vein endothelial cells (HUVECs) were used at passages 3-6. For analysis of reactive oxygen species (ROS), H_2O_2 (Thermo Fisher Scientific, Waltham, MA) and *N*-acetylcysteine (NAC; Calbiochem, San Diego, CA) were used as an ROS inducer and an ROS scavenger, respectively. To examine the effects of H_2O_2 on TSP-1 expression, HUVECs were seeded on 0.1% gelatin-coated culture plates and incubated overnight. Without change of medium, H_2O_2 was applied at final concentrations of 0.01, 0.05, and 0.1 mM and incubated for 10 minutes. For immunocytochemistry (ICC), HUVECs were plated into Lab-Tek Permanox slides precoated with 0.1% gelatin and incubated overnight. Then, the cells, with or without pretreatment with 30 mM of NAC for 60 minutes, were treated with 0.1 mM of H_2O_2 for 10 minutes.

To examine the effects of HUVEC-derived TSP-1 on TGF-β/Smad signaling and proliferation in primary hepatocyte cultures, primary hepatocytes were isolated from 8- to 12-week-old adult WT mouse livers using collagenase perfusion as previously described.[15] Isolated hepatocytes were plated on type I collagen (10-μg/mL)-coated dishes in Williams' E medium, supplemented with 5 μg/mL of insulin, 5 μg/mL of transferrin, 10 ng/mL of endothelial growth factor, 10^{-5} M aprotinin, 10^{-5} M of dexamethasone, 10^{-3} M of nicotinamide, and 10% fetal bovine serum and incubated at 37°C for 24 hours. To examine the effect of HUVEC-derived TSP-1 on TGF-β/Smad signaling in hepatocytes, the conditioned media from HUVECs (treated with 1.0 mM of H_2O_2 for 2 hours) were added to primary hepatocytes with or without pretreatment of 5 μM of LSKL or SLLK peptide (GenScript, Piscataway, NJ),[16,17] cultured for an additional 4 hours, and the cells were used for the analysis. To examine the effect of HUVEC-derived TSP-1 on hepatocyte proliferation, the conditioned media from HUVECs were added to primary hepatocytes, cultured for an additional 24 hours, and the cells were used for the analysis.

Data Presentation and Statistical Analysis. All experiments were performed in triplicate, and the data shown are representative of results consistently observed. Data are expressed as the mean ± standard deviation. Data analysis was performed with SPSS 12.0.1 for Windows (SPSS, Inc., Chicago, IL). Statistical analyses were performed using the Student *t* test or analysis of variance, followed by Bonferroni's multiple comparison tests, when appropriate. A P value of <0.05 was considered significant.

Results

PH Induces an Immediate and Prominent Induction of TSP-1 mRNA and Protein in the Regenerating Liver. An intact liver in adult mice expresses nearly undetectable levels of *TSP-1* mRNA.[12] We first determined whether PH could trigger TSP-1 induction in the regenerating liver. *TSP-1* mRNA was immediately induced, with a peak at 3 hours after hepatectomy, in WT mice by real-time PCR (Fig. 1A). TSP-1 protein was also induced, reaching a peak at ~6 hours (Fig. 1B). Those mRNA and protein levels returned to basal levels by 24 hours (Fig. 1A,B). Thus, PH induced immediate and transient TSP-1 expression in the initial phase of liver regeneration. Secondary minor inductions of *TSP-1* mRNA and protein were found to peak at 48 and 72 hours, respectively (Fig. 1A,B).

We next determined the cellular source of TSP-1 by immunostaining. In the intact liver, the expression of TSP-1 protein was detectable only in platelets with GPIIb/IIIa expression by double IF staining (Fig. 1C). The tissue distribution of TSP-1 protein localized in the sinusoid at 6 and 72 hours after PH (Fig. 1D), suggesting that cells localized in the sinusoid (e.g., endothelial cells [ECs], Kupffer cells, and hepatic stellate cells; HSCs) are responsible for newly synthesized TSP-1 in the regenerating liver. Double IF staining revealed that TSP-1 protein predominantly colocalized with platelet/endothelial cell adhesion molecule-1 (PECAM-1)/cluster of differentiation (CD)31 (an EC marker) at 6 hours in the regenerating liver (Fig. 2A). In contrast, TSP-1 protein at 6 hours did not colocalize with either F4/80 (a Kupffer cell marker) or alpha smooth muscle actin (α-SMA; a marker for myofibroblasts, such as activated HSCs) (Fig. 2A). The activation peak of HSCs is at 72 hours after PH[18] and many α-SMA-positive cells were observed (Supporting Fig. 1). At 72 hours, however, TSP-1 protein did

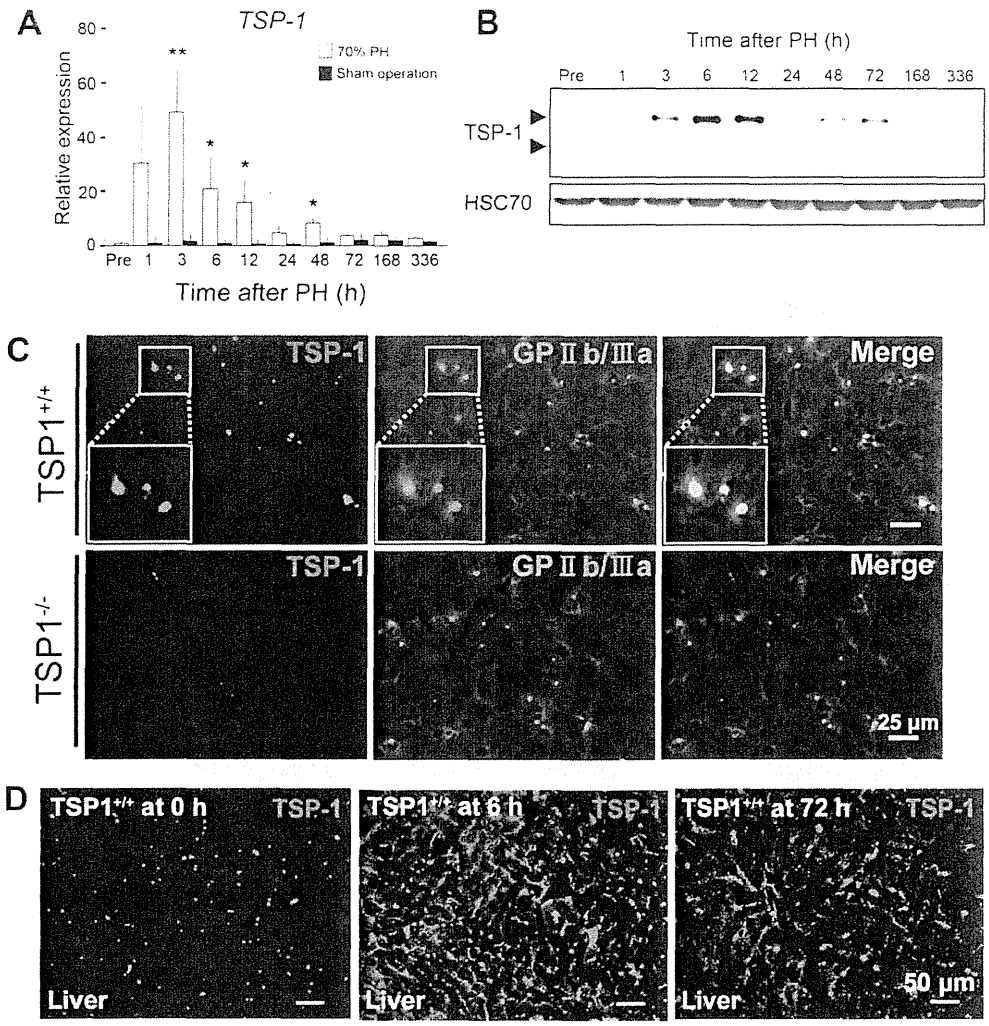

Fig. 1. An immediate and significant induction of *TSP-1* mRNA and protein in response to PH. (A) Real-time PCR analysis of *TSP-1* mRNA expression after 70% PH (n = 8 per time point) versus sham operation (n = 3 per time point). Data were normalized to the amount of *18S ribosomal* RNA serving as the internal control. $^{*}P < 0.05$ versus sham-operated mice; $^{**}P < 0.01$ versus sham-operated mice. (B) Western blotting analysis of TSP-1 protein expression in the regenerating liver. Heat shock cognate protein 70 (HSC70) served as a loading control. (C) Double IF staining of TSP-1 (red) and GPIIb/IIIa (green) at 0 hours in WT ($TSP1^{+/+}$) and TSP-1-null ($TSP1^{-/-}$) liver. Note that the distribution of TSP-1 in the intact WT liver shows only in platelets, as evidenced by colocalization of TSP-1 with the platelet marker, GPIIb/IIIa (yellowish dots in the merged image). Scale bar = 50 μm. (D) IF staining for TSP-1 in WT liver at 0, 6, and 72 hours after PH. Scale bar = 50 μm.

colocalize with PECAM-1/CD31 and α-SMA, but not with F4/80 (Fig. 2B). Indeed, it is known that activated HSCs express TSP-1 and thereby activate the TGF-β-signaling pathway *in vitro*.[19] These results suggest that ECs are the major source of TSP-1 expression in the initial phase at 6 hours, whereas ECs and activated HSCs participate in secondary TSP-1 expression at 72 hours. As noted above, immediate early genes are genes that are rapidly, but transiently (within approximately the first 4 hours), activated in response to hepatectomy.[1,2] Thus, TSP-1 produced by ECs is a novel candidate immediate early gene in the initial response to PH.

TSP-1 Deficiency Accelerates a Liver Regeneration After PH, but Does Not Affect the Termination Phase. Because immediate early genes play a significant role in the regulation of cell growth in the regenerating liver,[1,2] we next examined the involvement of TSP-1 in the control of liver regeneration. The rates of recovery of liver mass and of cell proliferation after PH were compared between WT and TSP-1-null mice. TSP-1-null mice showed significantly faster recovery of liver:body-weight ratio from day 1 to day 7 after surgery, compared with controls ($P < 0.05$ at 24, 48, and 168 hours and $P < 0.01$ at 72 hours; Fig. 3A). However, no excess liver mass had been gained at day

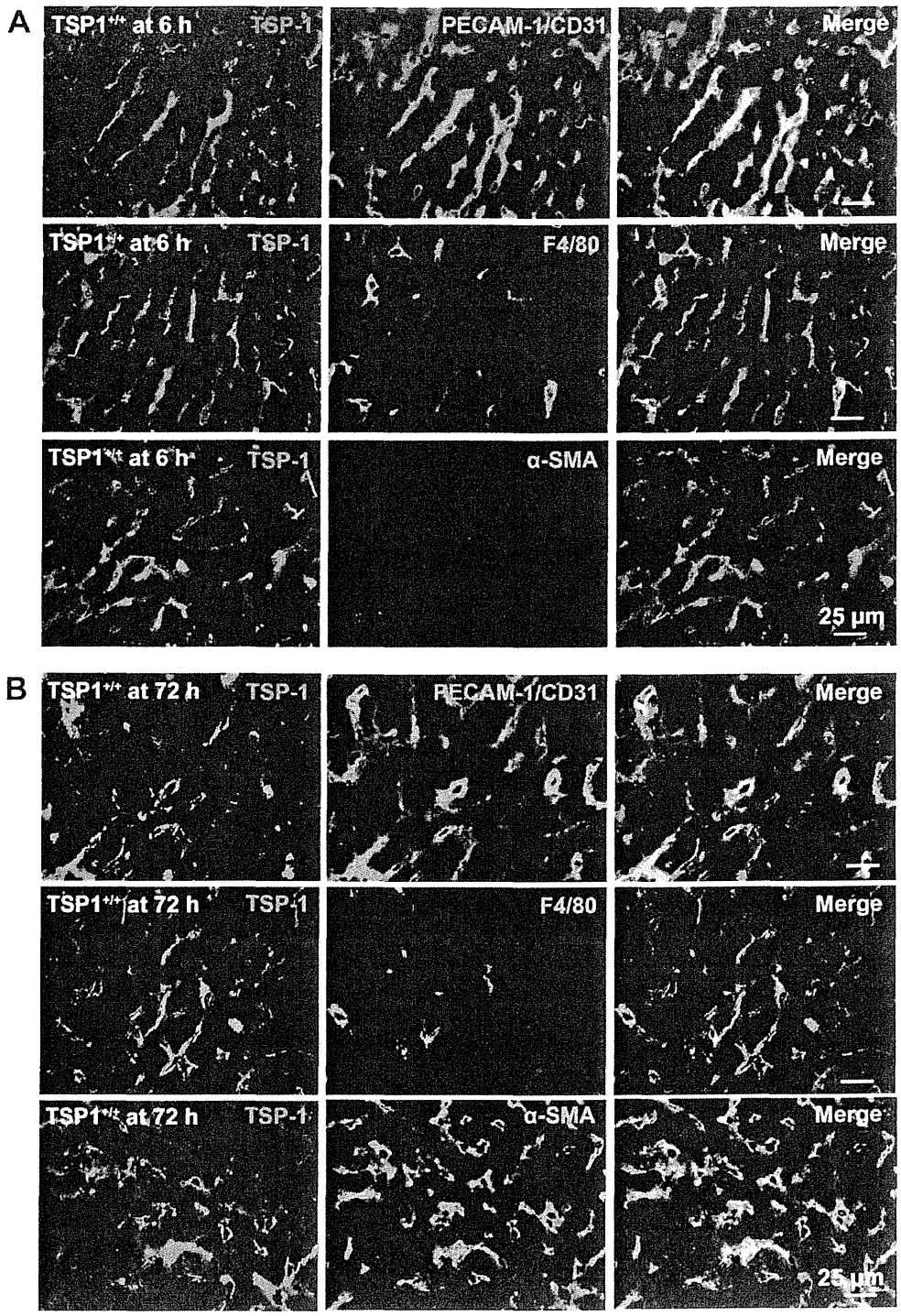

Fig. 2. Tissue distribution of TSP-1 protein in the regenerating liver. (A and B) TSP-1 expression at 6 (A) and 72 hours (B) after PH. Double IF staining for TSP-1/PECAM-1 (CD31), TSP-1/F4/80, and TSP-1/α-SMA at 6 and 72 hours in WT mice (TSP-1, red; PECAM-1 [CD31], F4/80, and α-SMA, green). Scale bar = 25 μm.

14 in TSP-1-null mice, compared with controls. Next, cell proliferation was evaluated using a BrdU incorporation assay (a marker for the S phase of the cell cycle). The proliferation peaks of hepatocytes and nonparenchymal cells after PH occurred at ~36-48 and 72 hours, respectively.[2,4,14] Although only a few

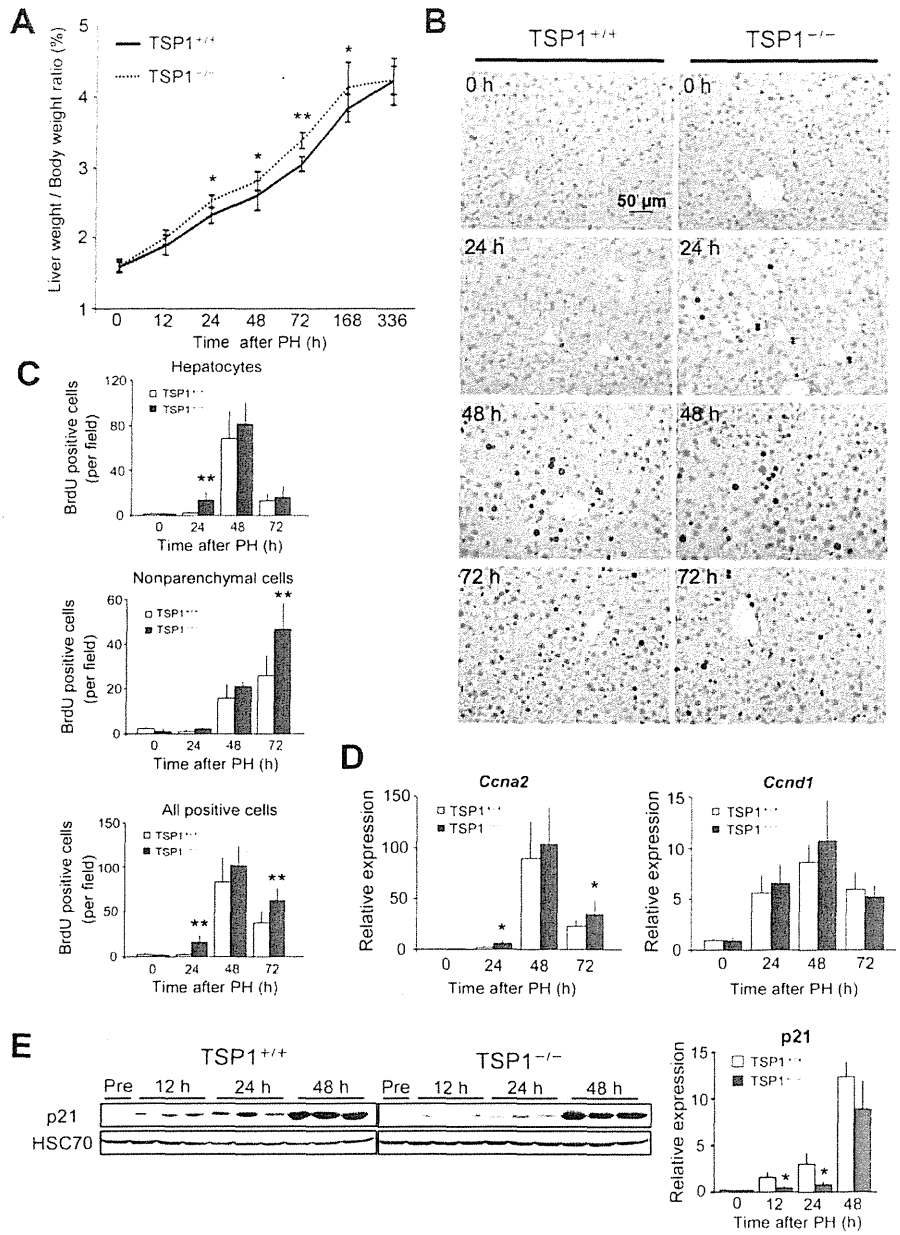

Fig. 3. Accelerated liver regeneration with down-regulation of p21 protein expression in TSP-1-null mice after PH. (A) Assessment of restoration of liver mass. Liver:body-weight ratio was measured after PH (n = 10 per time point in each group). $*P < 0.05$ versus *TSP-1*$^{+/+}$ mice; $**P < 0.01$ versus *TSP-1*$^{+/+}$ mice. (B and C) Assessment of BrdU incorporation in the regenerating liver. (B) IHC of BrdU in the regenerating liver. Arrowheads indicate BrdU-positive hepatocyte nuclei (brown) at 24 hours. Scale bar = 50 μm. (C) The number of BrdU-positive hepatocytes, nonparenchymal cells, and all positive cells (n = 10 per time points in each group). $**P < 0.01$ versus *TSP-1*$^{+/+}$ mice. (D) Real-time PCR analysis of *cyclin A2* (*Ccna2*) and *cyclin D1* (*Ccnd1*) mRNA expression in the regenerating liver (n = 10 per time point in each group). $*P < 0.05$ versus *TSP-1*$^{+/+}$ mice. (E) Assessment of p21 protein expression in the regenerating liver. Left panels: western blotting analysis of p21 protein expression in WT versus TSP-1-null liver. HSC70 was used as a loading control. Right panel: densitometric analysis of p21 protein expression (n = 3). Each p21 intensity was normalized to HSC70, then the intensity of WT mice at 0 hours was set to 1. $*P < 0.05$ versus *TSP-1*$^{+/+}$ mice. HSC70, heat shock cognate protein 70.

BrdU-positive hepatocytes were detectable at 24 hours in WT mice, TSP-1-null mice showed a significantly increased number of BrdU-positive hepatocytes (8-fold over controls) ($P < 0.01$; Fig. 3B,C). The number of BrdU-positive nonparenchymal cells in TSP-1-null mice significantly increased (2-fold) at 72 hours, compared with controls ($P < 0.01$; Fig. 3C). Total proliferative activity (of hepatocytes and

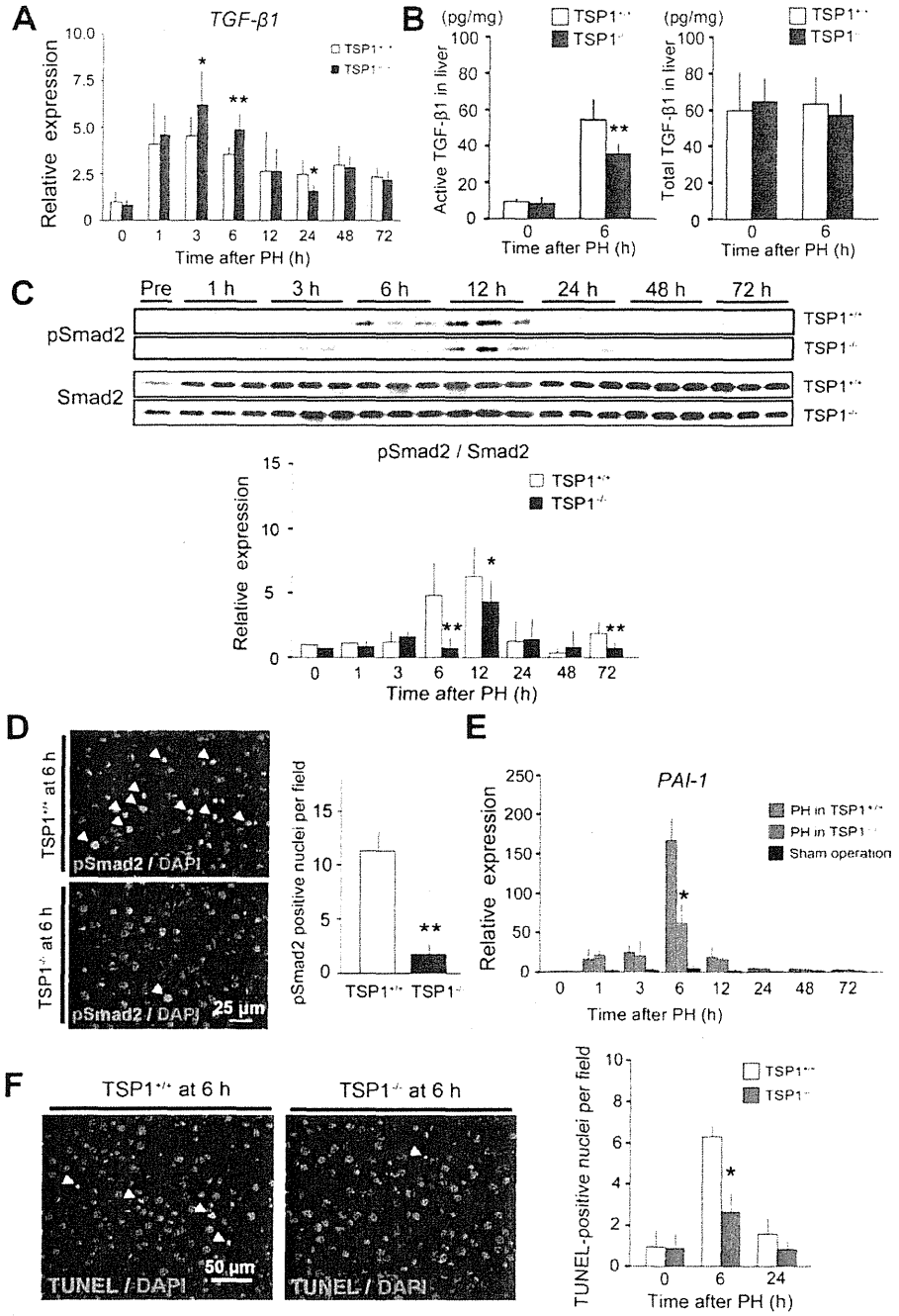

Fig. 4. Significantly decreased TGF-β/Smad signal transduction and cell death in TSP-1-null mice after PH. (A) Real-time PCR analysis of *TGF-β1* mRNA expression after PH (n = 8 per time point in each group). $*P < 0.05$ versus *TSP-1*$^{+/+}$ mice; $**P < 0.01$ versus *TSP-1*$^{+/+}$ mice. (B) Levels of active and total TGF-β1 in WT and TSP-1-null liver at 6 hours after PH (n = 6 per time point in each group). $**P < 0.01$ versus *TSP-1*$^{+/+}$ mice. (C-E) Effects of TSP-1 deficiency on pSmad2 expression in the regenerating liver. (C) Upper panels: western blotting analysis of pSmad2 and total Smad2 in WT and TSP-1-null liver. Lower panel: densitometric analysis of pSmad2 protein expression (n = 3). Each pSmad2 intensity was normalized to total Smad2, then the intensity of WT mice at 0 hours was set to 1. $*P < 0.05$ versus *TSP-1*$^{+/+}$ mice; $**P < 0.01$ versus *TSP-1*$^{+/+}$ mice. (D) Assessment of pSmad2 nuclear localization. Left panel: IF staining for pSmad2 at 6 hours in WT and TSP-1-null liver. Right panel: analysis of pSmad2-positive nuclei (n = 5 in each group). Arrowheads indicate pSmad2 (red)/ DAPI (blue) double-positive nuclei (purple). $**P < 0.01$ versus *TSP-1*$^{+/+}$ mice. Scale bar = 25 μm. (E) Real-time PCR analysis of *PAI-1* mRNA expression in WT and TSP-1-null liver after PH (n = 8 per time point in each group) and in WT liver after sham operation (n = 3 per time point). $**P < 0.01$ versus *TSP-1*$^{+/+}$ mice. (F) Assessment of TUNEL-positive cell death in the regenerating liver. Left panel: TUNEL staining at 6 hours after PH in WT and TSP-1-null liver. Right panel: analysis of TUNEL-positive cells (n = 5 per time point in each group). Arrowheads indicate TUNEL (red)/DAPI (blue) double-positive nuclei (purple). $**P < 0.01$ versus *TSP-1*$^{+/+}$ mice. Scale bar = 50 μm. DAPI, 4′,6-diamidino-2-phenylindole.

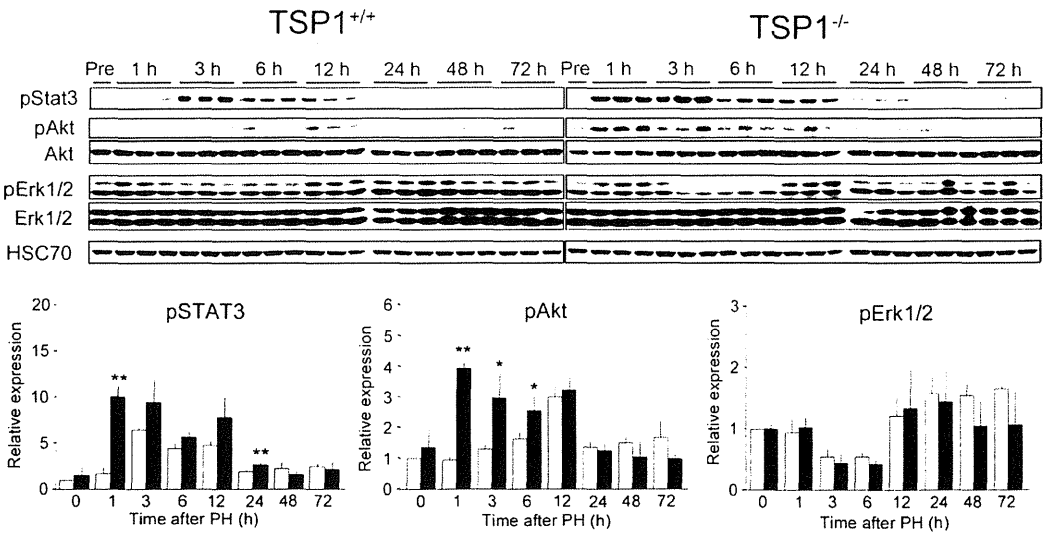

Fig. 5. TSP-1 deficiency enhances STAT3 and PI3K/Akt, but not Erk1/2 signal, in the early phase after PH. Upper panels: western blotting analysis of STAT3, PI3K/Akt, and Erk1/2 signals. HSC70 served as a loading control. Lower panels: densitometric analysis of phosphorylated protein expression after PH. Each pSTAT3, pAkt, and pErk1/2 intensity was normalized to HSC70, then the intensity of WT mice at 0 hours was set to 1. $*P < 0.05$ versus *TSP-1*$^{+/+}$ mice; $**P < 0.01$ versus *TSP-1*$^{+/+}$ mice.

nonparenchymal cells) in TSP-1-null mice was significantly higher at 24 and 72 hours, compared with controls ($P < 0.01$ in both; Fig. 3C).

Cyclins are required for cell-cycle progression. The mRNA levels of cyclin A2 (*Ccna2*) and cyclin D1 (*Ccnd1*) increase and peak in S phase and early to mid G_1 phase, respectively. Expression levels of *Ccna2* mRNA in TSP-1-null mice were significantly higher at 24 (2.3-fold) and 72 hours (1.5-fold), compared with controls ($P < 0.05$ in both; Fig. 3D). Although *Ccnd1* mRNA levels increased and peaked at 48 hours in both WT and TSP-1-null mice, there was no significant difference between them (Fig. 3D). The cyclin-dependent kinase inhibitor, p21, plays a critical role in the inhibition of hepatocyte proliferation at the G_1/S transition of the cell cycle *in vivo*.[20] Induction levels of p21 protein in TSP-1-null mice significantly diminished at 12 and 24 hours, compared with controls (70% less than that of controls, both at 12 and 24 hours; $P < 0.05$ in both), whereas p21 showed at similar levels at 48 hours in WT and TSP-1-null liver (Fig. 3E). These results suggest that TSP-1 is a negative regulator of liver regeneration after PH, and that TSP-1 deficiency accelerates the S-phase entry of hepatocytes by down-regulation of p21 protein expression. However, TSP-1 does not affect the termination phase of liver regeneration after PH.

TGF-β/Smad Signaling Is Activated by TSP-1 in Response to PH. To address the possible mechanisms underlying this accelerated liver regeneration in TSP-1-null mice, we examined TGF-β/Smad signaling. *TGF-β1* mRNA levels in both WT and TSP-1-null mice increased after hepatectomy by real-time PCR, and those levels in TSP-1-null mice were significantly up-regulated at 3 and 6 hours, compared with controls ($P < 0.05$ at 3 hours and $P < 0.01$ at 6 hours; Fig. 4A). In sharp contrast, the levels of active TGF-β1 in TSP-1-null liver were significantly lower than controls at 6 hours after PH, whereas the levels of total TGF-β1 did not show any significant differences between them (Fig. 4B). Furthermore, the levels of phosphorylated Smad2 (pSmad2, C-terminal Ser465/467) protein, as a downstream mediator of active TGF-β1, significantly diminished at 6 and 12 hours in TSP-1-null mice, compared with controls (to 16% at 6 hours and 69% at 12 hours versus controls, respectively; $P < 0.01$ at 6 hours and $P < 0.05$ at 12 hours), as determined by western blotting (Fig. 4C). Using IF staining, we confirmed the significantly decreased number of nuclear localized pSmad2-positive cells at 6 hours in TSP-1-null mice, compared with controls ($P < 0.01$; Fig. 4D). A secondary, minor induction of pSmad2 at 72 hours was also significantly attenuated in TSP-1-null mice, compared with controls (Fig. 4C).

Plasminogen activator inhibitor-1 (PAI-1) is one of the downstream targets of TGF-β1 in hepatocytes.[21] Although intense inductions of *PAI-1* mRNA at 6 hours after hepatectomy were observed in both WT mice and TSP-1-null mice by real-time PCR, the induction level in TSP-1-null mice was significantly diminished (to 37% of controls; $P < 0.05$ at 6 hours) (Fig. 4E).

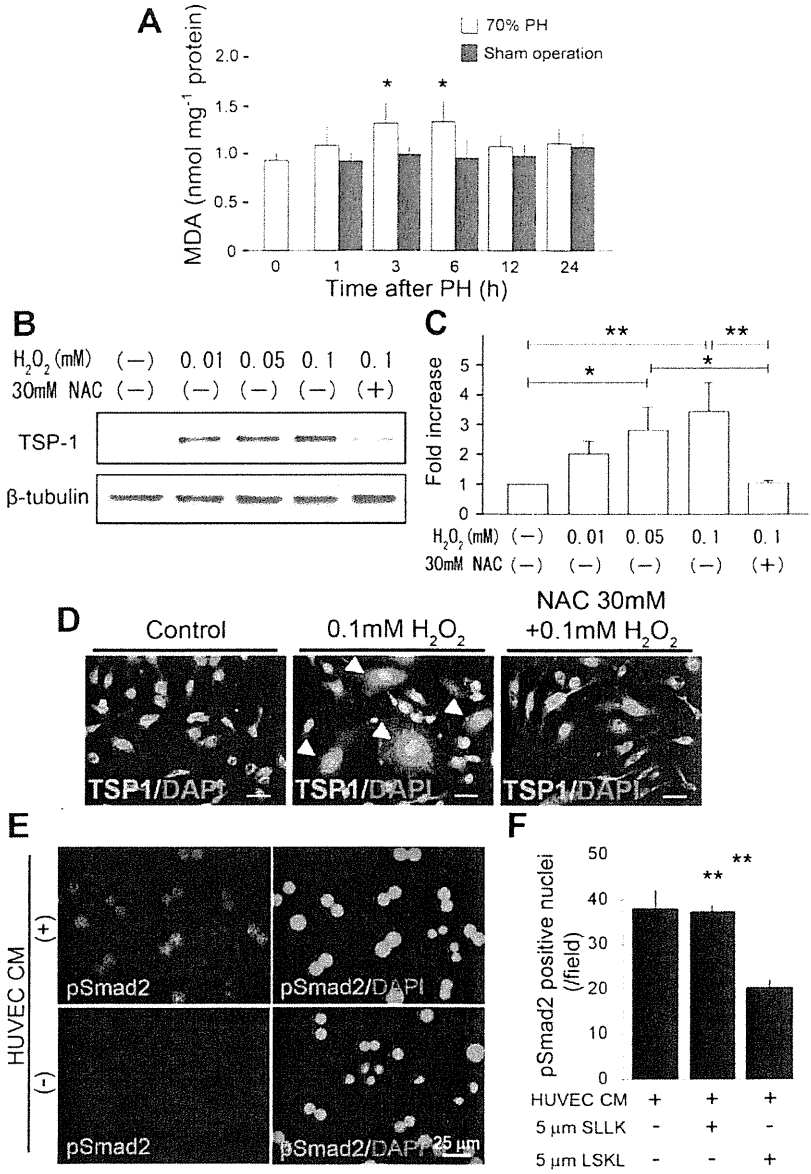

Fig. 6. TSP-1 induction in ECs by ROS. (A) Assessment for levels of MDA after 70% PH (n = 5) and sham operation (n = 3). *$P <$ 0.05 versus sham-operated mice. (B-D) TSP-1 protein expression by H_2O_2, a potent ROS inducer, in HUVECs. (B) Western blotting analysis of TSP-1 after treatment of HUVECs with H_2O_2. β-tubulin served as a loading control. (C) Densitometric analysis of TSP-1 expression from three independent experiments. Each TSP-1 intensity was normalized to β-tubulin, then the intensity of control was set to 1. Note that the TSP-1 protein expression levels after treatment with 0.05 and 0.1 mM of H_2O_2 are significantly higher versus controls, whereas the induction of TSP-1 by treatment with 0.1 mM of H_2O_2 is significantly inhibited with a pretreatment using 30 mM of NAC. *$P < 0.05$; **$P < 0.01$. (D) ICC for TSP-1 protein in HUVECs after treatment with H_2O_2 (TSP-1, green; DAPI, blue). Note that HUVECs after treatment with 0.1 mM of H_2O_2 express TSP-1 in their cytoplasm (arrowheads), whereas the induction of TSP-1 is inhibited by pretreatment using 30 mM of NAC. Scale bar = 50 μm. (E and F) Assessment of pSmad2 nuclear localization in primary hepatocytes. (E) IF staining for pSmad2 with or without ROS-treated CM from HUVECs (HUVEC CM). Scale bar = 25 μm. (F) Effect of TSP-1-inhibitory peptide LSKL on pSmad2 induction. Error bars represent standard deviation (n = 5 in each group; field = 0.15 mm^2). SLLK, control peptide. **$P < 0.01$. DAPI, 4′,6-diamidino-2-phenylindole.

Cell death is also implicated as a mechanism of TGF-β-mediated cell-growth inhibition. TUNEL-positive cells, as a marker for cell death, are immediately and transiently detectable after hepatectomy.[22] We determined whether deficiency in TSP-1 affected cell death in the regenerating liver. Although the number of TUNEL-positive cells in WT liver transiently increased at 6 hours after hepatectomy, TSP-1-null liver showed a significant reduction, compared with controls ($P < 0.05$ at 6 hours; Fig. 4F).

These results suggest that TSP-1-mediated active TGF-β1 plays a pivotal role in TGF-β/Smad signal transduction after PH.

Deficiency in TSP-1 Accelerates STAT3 and PI3K/Akt Signals, Not Extracellular Signal-Related Kinase 1 And 2 Signal, in the Early Phase After PH. There is *in vitro* evidence that TSP-1 down-regulates phosphorylated Akt (Ser473) expression through its receptor, CD47, in HUVECs.[23] Indeed, signaling pathways, such as phosphatidylinositide 3-kinase (PI3K)/Akt, signal transducer and activator of transcription 3 (STAT3), and extracellular signal-related kinase 1 and 2 (Erk1/2), are important for cell survival and/or proliferation after PH.[24] Therefore, we next examined whether the deficiency in TSP-1 affected the activation of these signaling pathways in the early phases po

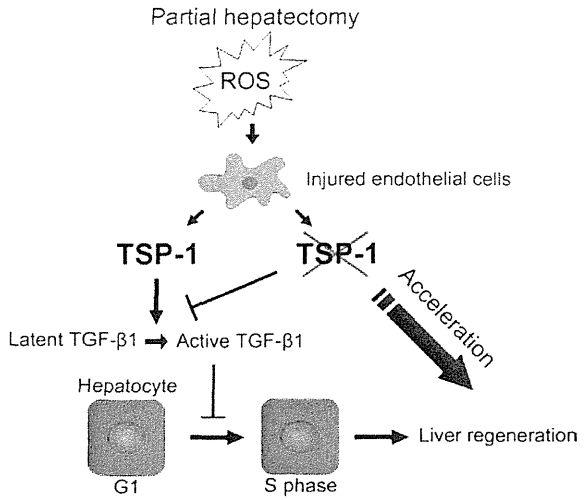

Fig. 7. Schematic illustration of the role of TSP-1 in the regenerating liver. In WT mice, newly synthesized ROS in response to PH stimulate ECs to express TSP-1. TSP-1 induced by ECs converts latent TGF-β1 into its active form. Active TGF-β1 suppresses cell-cycle progression in hepatocytes at the G_1/S checkpoint. In contrast, TSP-1 deficiency decreases active TGF-β1 levels, which, in turn, results in the acceleration of liver regeneration.

hepatectomy. TSP-1-null mice showed earlier, more intense phosphorylation of STAT3 (Tyr705) (6-fold at 1 hour; $P < 0.01$) and Akt (Ser473) (4.2-fold at 1 hour; $P < 0.01$) in the early stage after PH, compared with controls, as determined by western blotting (Fig. 5). In contrast, levels of phosphorylated Erk1/2 did not show any remarkable differences between the two groups (Fig. 5).

TSP-1 Induction in ECs Is Associated With ROS. Although our findings show that TSP-1 plays a potential role as a negative regulator in the regenerating liver, the mechanism of TSP-1 induction in ECs in response to PH remains unknown. There is a line of evidence that ROS are produced in the regenerating liver after PH.[22,25] In WT mice, levels of tissue content of MDA as a lipid peroxidation marker for ROS generation were significantly increased at both 3 and 6 hours and returned to basal levels by 12 hours after hepatectomy ($P < 0.05$ in both; Fig. 6A). Next, to determine whether ROS could induce TSP-1 expression in ECs, we performed an *in vitro* study using HUVECs with the potent ROS inducer, H_2O_2. In HUVECs, treatment with H_2O_2 induced TSP-1 protein expression in a dose-dependent manner (Fig. 6B-D). Furthermore, this induction was inhibited by pretreatment with 30 mM of NAC, a scavenger of ROS (Fig. 6B-D). Thus, these results indicate that oxidative stress is one factor responsible for TSP-1 induction in ECs.

To further determine whether HUVEC-derived TSP-1 could modulate TGF-β/Smad signaling and proliferation in hepatocytes *in vitro*, we isolated primary hepatocytes from adult WT mice.[15] The treatment of conditioned media from HUVECs with primary hepatocytes actually induced pSmad2 (Fig. 6E). Furthermore, the pretreatment of primary hepatocytes with TSP-1-inhibitory peptide LSKL[16,17] significantly suppressed conditioned media (CM)-induced pSmad2 expression, whereas the control peptide, SLLK, showed no effects (Fig. 6F). It is known that primary hepatocytes lack the ability to proliferate, even though such cells *in vivo* readily replicate and/or synthesize DNA after PH.[26] Although a few proliferative primary hepatocytes were found by Ki67 immunostaining in culture, the treatment of CM from HUVECs with primary hepatocytes significantly reduced the number of Ki67-positive cells (Supporting Fig. 2).

Discussion

In the present study, we have demonstrated the following (Fig. 7): (1) TSP-1 is induced in ECs as an immediate early gene by ROS and participates in TGF-β signal transduction in the initial response to PH and (2) TSP-1 deficiency results in the significant reduction of TGF-β/Smad signal, and this could cause the accelerated S-phase entry of hepatocytes by down-regulation of p21 protein expression. Thus, this is the first study providing compelling evidence that local TGF-β activation machinery plays an important role in inhibiting liver regeneration after PH.

Our study supports the notion that oxidative stress is one factor responsible for TSP-1 induction in the regenerating liver. TSP-1 is the most likely candidate protein induced by oxidative stress in proteomic analysis using brain ECs.[27] These findings imply that ECs initially sense locally produced ROS in response to tissue damage, and that the subsequent induction of TSP-1 in these cells after initiates tissue remodeling. Indeed, our results revealed that EC-derived TSP-1 can modulate TGF-β/Smad signaling and proliferation in hepatocytes. ECs represent the largest population of nonparenchymal cells in the liver. Identification of the functional role of immediate early genes provides the clues for understanding the molecular bases of liver regeneration. One recent study documented that Id-1, a vascular endothelial growth factor-A receptor (VEGFR)-2-mediated transcriptional factor, was induced in ECs at ~48 hours after hepatectomy; Id-1, in turn, promoted hepatocyte proliferation.[28] There has, as yet, been no report implicating ECs in earlier

stages of the regenerating liver (within 24 hours). We have identified TSP-1 as a novel immediate early gene derived from ECs, showing that the expression level of TSP-1 was immediately up-regulated and returned to basal levels by 24 hours in response to PH. Our findings and the previous report[28] suggest that ECs may play two distinct roles in hepatocyte proliferation after PH: One is an antiproliferative role by activating the TSP-1/TGF-β1 axis within 24 hours, and the other is a proproliferative role by activating VEGFR-2 after 24 hours. This finding is consistent with the evidence that TSP-1 inhibits the activation of VEGFR-2 through its receptor, CD47, in ECs,[23] and suggests that the reduction of TSP-1 expression may be required for the functional shift in ECs from an anti- to a proproliferative role in hepatocytes. Microvascular rearrangement is important for tissue remodeling, and the antiangiogenic action is one of the well-recognized functions of TSP-1.[29] However, the expression of CD31 mRNA for monitoring angiogenesis did not show any significant difference between WT and TSP-1-null mice at 24, 48, and 72 hours after PH (Hayashi H, and Sakai T; unpublished data), suggesting that TSP-1 does not affect vascularization during liver regeneration after PH.

TGF-β1 is known to be a potent inhibitor of mitogen-stimulated DNA synthesis in cultured hepatocytes.[3] p21 is important for inhibiting hepatocyte proliferation *in vivo*, especially at the G_1/S transition of the cell cycle,[20] and the expression of p21 is up-regulated by TGF-β1.[30] There is evidence that *TGF-β1* mRNA induction occurs within 4 hours and remains elevated until 72 hours after PH.[5,6] In contrast, we found the only limited activation of TGF-β signaling in an earlier phase (within 24 hours), with a peak at ~12 hours. It is known that TGF-β is secreted as latent forms and they are converted into active TGF-β in response to injury. There are several mechanisms for activation, such as by proteases, integrins (e.g., $\alpha v\beta 6$ and $\alpha v\beta 8$), and TSP-1, all of which are likely to be tissue specific.[31] Whereas the complete lack of TGF-β-mediated signal in hepatocyte-specific *TGF-β type II receptor* knockout mice accelerates hepatocyte proliferation in the later phase (~36-48 hours) after hepatectomy,[7] the role of TGF-β signaling in the earlier phase (within 24 hours) remains to be elucidated. Our present findings provide compelling evidence that locally activated TGF-β1 mediated by TSP-1 as an immediate early gene is critical in the early phase (within 24 hours) post PH to initiate the inhibitory effect on hepatocyte proliferation, and this TGF-β signaling has a functional link to the G_1/S-phase transition by modulating p21 protein expression. A major downstream target of TGF-β1, PAI-1,[21] is a negative regulator of liver regeneration, and PAI-1-null mice show acceleration of liver regeneration after Fas-mediated massive hepatocyte death.[32] The significant down-regulation of PAI-1 expression in our TSP-1-null liver may be implicated in the accelerated hepatocyte proliferation after PH. However, our TSP-1-null model did not show any obvious differences in the termination phase of liver regeneration, compared with controls, such as the *TGF-β type II receptor* knockout mice model.[7] Although the molecular mechanisms underlying the termination of liver regeneration remain to be elucidated,[4] our and other findings suggest that the orchestrating interactions among positive and negative regulators in hepatocyte proliferation would be critical for the termination of liver regeneration.[4,24]

Active TGF-β1 induces hepatocyte cell death. STAT3- and PI3K/Akt-signaling pathways are crucial for cell survival (i.e., antiapoptosis) in the acute phase after PH. Our signaling data using TSP-1-null mice are consistent with previous findings showing that STAT3- and PI3K/Akt-signaling pathways, but not the Erk1/2 pathway, play a protective role against TGF-β-induced apoptosis in hepatocyte cell lines.[33,34] Several *in vitro* studies have reported that TSP-1 down-regulates phosphorylated Akt expression in retina[35] and ECs.[23] Another *in vitro* study showed that the lack of TSP-1 in retinal ECs results in up-regulation of phosphorylated Akt expression, but not phosphorylated Erk1/2.[36] Because TSP-1 is a multidomain and multifunctional matricellular protein, our data and these findings suggest that TSP-1 modulates not only TGF-β signal, but also cell survival signals, such as STAT3 and PI3K/Akt signals, through its multidomain.

In the clinical setting, no established therapeutic strategies to accelerate liver regeneration have been available, to date. The inhibition of TSP-1 function attenuates locally activated TGF-β1 signals and thereby accelerates hepatocyte proliferation; hence, TSP-1 could be a novel therapeutic target for accelerating liver regeneration after PH.

Acknowledgments: The authors thank Dr. Jack Lawler for TSP-1-null mice, Drs. Koichi Matsuzaki and Deane Mosher for antibodies, and Diskin Erb and Dr. Judy Drazba (Imaging Core, Lerner Research Institute, Cleveland, OH) for IF microscopic analyses. The authors are also grateful to Dr. Jo Adams for assistance with TSP-1 immunostaining experiments and scientific discussions.

References

1. Taub R. Liver regeneration 4: transcriptional control of liver regeneration. FASEB J 1996;10:413-427.
2. Fausto N. Liver regeneration. J Hepatol 2000;32:19-31.
3. McMahon JB, Richards WL, de Campo AA, Song MK, Thorgeirsson SS. Differential effects of transforming growth factor-beta on proliferation of normal and malignant rat liver epithelial cells in culture. Cancer Res 1986;46:4665-4671.
4. Michalopoulos GK. Liver regeneration. J Cell Physiol 2007;213: 286-300.
5. Jakowlew SB, Mead JE, Danielpour D, Wu J, Roberts AB, Fausto N. *Transforming growth factor-beta (TGF-beta) isoforms in rat liver regeneration*: messenger RNA expression and activation of latent TGF-beta. Cell Regul 1991;2:535-548.
6. Braun L, Mead JE, Panzica M, Mikumo R, Bell GI, Fausto N. Transforming growth factor beta mRNA increases during liver regeneration: a possible paracrine mechanism of growth regulation. Proc Natl Acad Sci U S A 1988;85:1539-1543.
7. Oe S, Lemmer ER, Conner EA, Factor VM, Levéen P, Larsson J, et al. Intact signaling by transforming growth factor beta is not required for termination of liver regeneration in mice. Hepatology 2004;40: 1098-1105.
8. Mosher DF. Physiology of thrombospondin. Annu Rev Med 1990;41: 85-97.
9. Crawford SE, Stellmach V, Murphy-Ullrich JE, Ribeiro SM, Lawler J, Hynes RO, et al. Thrombospondin-1 is a major activator of TGF-beta1 *in vivo*. Cell 1998;93:1159-1170.
10. Adams JC. Thrombospondins: multifunctional regulators of cell interactions. Annu Rev Cell Dev Biol 2001;17:25-51.
11. Kyriakides TR, Maclauchlan S. The role of thrombospondins in wound healing, ischemia, and the foreign body reaction. J Cell Commun Signal 2009;3:215-225.
12. Lawler J, Sunday M, Thibert V, Duquette M, George EL, Rayburn H, Hynes RO. Thrombospondin-1 is required for normal murine pulmonary homeostasis and its absence causes pneumonia. J Clin Invest 1998;101:982-992.
13. Moriya K, Bae E, Honda K, Sakai K, Sakaguchi T, Tsujimoto I, et al. A fibronectin-independent mechanism of collagen fibrillogenesis in adult liver remodeling. Gastroenterology 2011;140:1653-1663.
14. Yuan H, Zhang H, Wu X, Zhang Z, Du D, Zhou S, et al. Hepatocyte-specific deletion of Cdc42 results in delayed liver regeneration after partial hepatectomy in mice. Hepatology 2009;49:240-249.
15. Yoshie M, Nishimori H, Lee GH, Ogawa K. High colony forming capacity of primary cultured hepatocytes as a dominant trait in hepatocarcinogenesis-susceptible and resistant mouse strains. Carcinogenesis 1998;19:1103-1107.
16. Ribeiro SM, Poczatek M, Schultz-Cherry S, Villain M, Murphy-Ullrich JE. The activation sequence of thrombospondin-1 interacts with the latency-associated peptide to regulate activation of latent transforming growth factor-beta. J Biol Chem 1999;274:13586-13593.
17. Meek RL, Cooney SK, Flynn SD, Chouinard RF, Poczatek MH, Murphy-Ullrich JE, Tuttle KR. Amino acids induce indicators of response to injury in glomerular mesangial cells. Am J Physiol Renal Physiol 2003;285:F79-F86.
18. Asai K, Tamakawa S, Yamamoto M, Yoshie M, Tokusashi Y, Yaginuma Y, et al. Activated hepatic stellate cells overexpress p75NTR after partial hepatectomy and undergo apoptosis on nerve growth factor stimulation. Liver Int 2006;26:595-603.
19. Breitkopf K, Sawitza I, Westhoff JH, Wickert L, Dooley S, Gressner AM. Thrombospondin 1 acts as a strong promoter of transforming growth factor beta effects via two distinct mechanisms in hepatic stellate cells. Gut 2005;54:673-681.
20. Albrecht JH, Poon RYC, Ahonen CL, Rieland BM, Deng C, Crary GS. Involvement of p21 and p27 in the regulation of CDK activity and cell cycle progression in the regenerating liver. Oncogene 1998;16: 2141-2150.
21. Westerhausen DR, Jr. Hopkins WE, Billadello JJ. Multiple transforming growth factor-beta-inducible elements regulate expression of the plasminogen activator inhibitor type-1 gene in Hep G2 cells. J Biol Chem 1991;266:1092-1100.
22. Lee FY, Li Y, Zhu H, Yang S, Lin HZ, Trush M, Diehl AM. Tumor necrosis factor increases mitochondrial oxidant production and induces *expression of uncoupling protein-2 in the regenerating mice* [correction of rat] liver. Hepatology 1999;29:677-687.
23. Kaur S, Martin-Manso G, Pendrak ML, Garfield SH, Isenberg JS, Roberts DD. Thrombospondin-1 inhibits VEGF receptor-2 signaling by disrupting its association with CD47. J Biol Chem 2010;285: 38923-38932.
24. Taub R. Liver regeneration: from myth to mechanism. Nat Rev Mol Cell Biol 2004;5:836-847.
25. Nakatani T, Inouye M, Mirochnitchenko O. Overexpression of antioxidant enzymes in transgenic mice decreases cellular ploidy during liver regeneration. Exp Cell Res 1997;236:137-146.
26. Tomomura A, Sawada N, Sattler GL, Kleinman HK, Pitot HC. The control of DNA synthesis in primary cultures of hepatocytes from adult and young rats: interactions of extracellular matrix components, epidermal growth factor, and the cell cycle. J Cell Physiol 1987;130:221-227.
27. Ning M, Sarracino DA, Kho AT, Guo S, Lee SR, Krastins B, et al. Proteomic temporal profile of human brain endothelium after oxidative stress. Stroke 2011;42:37-43.
28. Ding BS, Nolan DJ, Butler JM, James D, Babazadeh AO, Rosenwaks Z, et al. Inductive angiocrine signals from sinusoidal endothelium are required for liver regeneration. Nature 2010;468:310-315.
29. Zhang X, Lawler J. Thrombospondin-based antiangiogenic therapy. Microvasc Res 2007;74:90-99.
30. Albrecht JH, Meyer AH, Hu MY. Regulation of cyclin-dependent kinase inhibitor p21(WAF1/Cip1/Sdi1) gene expression in hepatic regeneration. Hepatology 1997;25:557-563.
31. Annes JP, Munger JS, Rifkin DB. Making sense of latent TGFbeta activation. J Cell Sci 2003;116:217-224.
32. Shimizu M, Hara A, Okuno M, Matsuno H, Okada K, Ueshima S, et al. Mechanism of retarded liver regeneration in plasminogen activator-deficient mice: impaired activation of hepatocyte growth factor after Fas-mediated massive hepatic apoptosis. Hepatology 2001;33: 569-576.
33. Chen RH, Su YH, Chuang RL, Chang TY. Suppression of transforming growth factor-beta-induced apoptosis through a phosphatidylinositol 3-kinase/Akt-dependent pathway. Oncogene 1998;17: 1959-1968.
34. Chen RH, Chang MC, Su YH, Tsai YT, Kuo ML. Interleukin-6 inhibits transforming growth factor-beta-induced apoptosis through the phosphatidylinositol 3-kinase/Akt and signal transducers and activators of transcription 3 pathways. J Biol Chem 1999;274: 23013-23019.
35. Sun J, Hopkins BD, Tsujikawa K, Perruzzi C, Adini I, Swerlick R, et al. Thrombospondin-1 modulates VEGF-A-mediated Akt signaling and capillary survival in the developing retina. Am J Physiol Heart Circ Physiol 2009;296:H1344-H1351.
36. Wang Y, Wang S, Sheibani N. Enhanced proangiogenic signaling in thrombospondin-1-deficient retinal endothelial cells. Microvasc Res 2006;71:143-151.

Published OnlineFirst May 2, 2012; DOI:10.1158/0008-5472.CAN-12-0299

Cancer Research

CD44s Regulates the TGF-β–Mediated Mesenchymal Phenotype and Is Associated with Poor Prognosis in Patients with Hepatocellular Carcinoma

Kosuke Mima, Hirohisa Okabe, Takatsugu Ishimoto, et al.

Cancer Res 2012;72:3414-3423. Published OnlineFirst May 2, 2012.

Published OnlineFirst May 2, 2012; DOI:10.1158/0008-5472.CAN-12-0299

CD44s Regulates the TGF-β–Mediated Mesenchymal Phenotype and Is Associated with Poor Prognosis in Patients with Hepatocellular Carcinoma

Kosuke Mima[1], Hirohisa Okabe[1], Takatsugu Ishimoto[1], Hiromitsu Hayashi[1], Shigeki Nakagawa[1], Hideyuki Kuroki[1], Masayuki Watanabe[1], Toru Beppu[1], Mayumi Tamada[2], Osamu Nagano[2], Hideyuki Saya[2], and Hideo Baba[1]

Abstract

The prognosis for individuals diagnosed with hepatocellular carcinoma (HCC) remains poor because of the high frequency of invasive tumor growth, intrahepatic spread, and extrahepatic metastasis. Here, we investigated the role of the standard isoform of CD44 (CD44s), a major adhesion molecule of the extracellular matrix and a cancer stem cell marker, in the TGF-β–mediated mesenchymal phenotype of HCC. We found that CD44s was the dominant form of CD44 mRNA expressed in HCC cells. Overexpression of CD44s promoted tumor invasiveness and increased the expression of vimentin, a mesenchymal marker, in HCC cells. Loss of CD44s abrogated these changes. Also in the setting of CD44s overexpression, treatment with TGF-β1 induced the mesenchymal phenotype of HCC cells, which was characterized by low E-cadherin and high vimentin expression. Loss of CD44s inhibited TGF-β–mediated vimentin expression, mesenchymal spindle-like morphology, and tumor invasiveness. Clinically, overexpression of CD44s was associated with low expression of E-cadherin, high expression of vimentin, a high percentage of phospho-Smad2–positive nuclei, and poor prognosis in HCC patients, including reduced disease-free and overall survival. Together, our findings suggest that CD44s plays a critical role in the TGF-β–mediated mesenchymal phenotype and therefore represents a potential therapeutic target for HCC. *Cancer Res; 72(13); 3414–23. ©2012 AACR.*

Introduction

Hepatocellular carcinoma (HCC) is the fifth most prevalent and the third most deadly type of cancer worldwide. In fact, it is diagnosed in more than half a million people worldwide each year (1). Surgical resection and liver transplantation are available options for the treatment of early-stage HCC; however, the prognosis of HCC remains poor because of a high level of tumor invasiveness, frequent intrahepatic spread, extrahepatic metastasis, and resistance to chemotherapy (2).

Epithelial–mesenchymal transition (EMT) has been shown to be a pivotal mechanism contributing to cancer invasion and metastasis including HCC (3–7) because epithelial cells lose their polarity and acquire the migratory properties of mesenchymal cells in the developmental process. In recent metastasis researches, EMT is also shown to play an important role in stem-like properties (8).

CD44, a major adhesion molecule of the extracellular matrix, has been implicated in a wide variety of physiologic processes, including leukocyte homing and activation, wound healing, and cell migration (9, 10). Cells produce CD44 protein isoforms through the process of alternative mRNA splicing. The CD44 standard isoform (CD44s) is expressed predominantly in hematopoietic cells and normal epithelial cell subsets, whereas the variant isoform (CD44v) is expressed by some epithelial cells during embryonic development, during lymphocyte maturation and activation, and by several types of carcinoma cells. Recently, cancer stem cells (CSC) in many tumors have been identified by positive expression of CD44, either individually or in combination with other markers, and these cells have been shown to be involved in tumor progression and metastasis (10–16). Although TGF-β signaling is a major regulator of EMT and it maintains the mesenchymal phenotype and stem cell states in an autocrine fashion in cancer (17), the underlying molecular mechanisms that integrate the mesenchymal phenotype with the EMT process and with CSC properties still remain unknown. Therefore, we hypothesize that CD44, a CSC marker, plays an important role in inducing EMT or in maintaining the mesenchymal phenotype in HCC.

Authors' Affiliations: [1]Department of Gastroenterological Surgery, Graduate School of Medical Sciences, Kumamoto University, Honjo, Kumamoto; and [2]Division of Gene Regulation, Institute for Advanced Medical Research, School of Medicine, Keio University, Shinanomachi, Shinjuku-ku, Tokyo, Japan

Note: Supplementary data for this article are available at Cancer Research Online (http://cancerres.aacrjournals.org/).

Corresponding Author: Hideo Baba, Department of Gastroenterological Surgery, Graduate School of Medical Sciences, Kumamoto University, 1-1-1 Honjo, Kumamoto 860-8556, Japan. Phone: 81-96-373-5212; Fax: 81-96-371-4378; E-mail: hdobaba@kumamoto-u.ac.jp

doi: 10.1158/0008-5472.CAN-12-0299

Published OnlineFirst May 2, 2012; DOI:10.1158/0008-5472.CAN-12-0299

Materials and Methods

Cell lines, culture conditions, and reagents

The human HCC lines PLC/PRF/5, HuH1, HLF, and HLE were purchased from the Japanese Collection of Research Bioresources. SK HEP-1 cells were purchased from American Type Culture Collection. The cells were routinely maintained in Dulbecco's Modified Eagle's Medium (Invitrogen) supplemented with 10% FBS (Invitrogen). The cells were incubated at 37°C in a 5% CO_2 air-humidified atmosphere. Purified recombinant human TGF-β1 (R&D Systems) was reconstituted in sterile 4 mmol/L HCl containing 1 mg/mL bovine serum albumin (Sigma). TGF-β1 was used at the indicated concentrations in serum-free medium.

Plasmids and siRNA transfection

The cDNA corresponding to human CD44s was introduced into the pcDNA3.1 expression plasmid (Invitrogen; ref. 18). PLC/PRF/5 cells were transfected with the resulting plasmids using Lipofectamine 2000 (Invitrogen). CD44 expression was transiently downregulated using a predesigned siRNA duplex directed against CD44, and a nontargeting siRNA was used as a negative control. The sequences of the siRNA (chimeric RNA–DNA) duplexes (Japan Bioservice) were as follows (18): CD44 siRNA, 5′-AAAUGGUCGCUACAGCAUCTT-3′ and 5′-GAUGCUGUAGCGACCAUUUTT-3′, and control siRNA, 5′-CGUACGCGGAAUACUUCGATT-3′ and 5′-UCGAAGUAUUCCGCGUACGTT-3′. HCC cells were transfected with the annealed siRNA for 24 to 72 hours using Lipofectamine 2000.

Protein extraction and Western blot analysis

Protein extraction from cultivated cells and Western blot analyses were carried out as previously described (19, 20). Briefly, the cells were lysed in cell lysis buffer containing 25 mmol/L Tris (pH 7.4), 100 mmol/L NaCl, and 1% Tween 20. Equal amount of proteins were loaded onto 10% gels and separated using SDS-PAGE. The resolved proteins were electrophoretically transferred to polyvinylidene fluoride membranes (Bio-Rad, Inc.). The membranes were blocked with 5% low-fat dry milk in TBS-T [25 mmol/L Tris (pH 7.4), 125 mmol/L NaCl, 0.4% Tween 20] for 1 hour at room temperature, followed by incubation with a primary antibody at 4°C overnight. The blots were extensively washed with TBS-T and incubated with an horseradish peroxidase (HRP)-conjugated secondary antibody diluted 1:2,000 in TBS-T for 1 hour at room temperature. The membranes were washed and visualized using a Chemiluminescent Detection Reagent Kit (ECL; GE Healthcare Corp.). Primary antibodies for E-cadherin (1:1,000 dilution; BD Transduction Laboratories), vimentin (1:1,000 dilution; Santa Cruz), CD44s (1:1,000 dilution; Bender MedSystems), phospho-Smad2 (1:500 dilution; Cell Signaling), Smad2/3 (1:1,000 dilution; Cell Signaling), and β-actin (1:1,000 dilution; Cell Signaling) were used for this study.

RNA extraction and quantitative reverse transcription PCR

Total RNA extraction, cDNA synthesis, and quantitative reverse transcription PCR (qRT-PCR) were carried out as previously described (19, 20). Total cellular RNA was extracted using the RNeasy Mini Kit (Qiagen), and cDNA was synthesized with the SuperScript III Transcriptor First Strand cDNA Synthesis System for RT-PCR (Invitrogen) according to the manufacturers' instructions. qRT-PCR was carried out using a LightCycler 480 II instrument (Roche). To determine the differences in the gene expression levels between specimens, the $2^{-\Delta\Delta C_t}$ method was used to measure the fold changes among the samples (21). To carry out qRT-PCR, primers were designed using the Universal Probe Library (Roche) following the manufacturer's recommendations. The primer sequences and probes used for real-time PCR were as follows: E-cadherin, 5′-TTGACGCCGAGAGCTACAC-3′, 5′-GTCGACCGGTGCAATCTT-3′, and universal probe #80; vimentin, 5′-TACAGGAAGCTGCTGGAAGG-3′, 5′-ACCAGAGGGAGTGAATCCAG-3′, and universal probe #13; CD44, 5′-GCAGTCAACAGTCGAAGAAGG-3′, 5′-TGTCCTCCACAGCTCCATT-3′, and universal probe #29; glyceraldehyde-3-phosphate dehydrogenase (GAPDH), 5′-AGCCACATCGCTCAGACAC-3′, 5′-GCCCAATACGACCAAATCC-3′, and universal probe #60; EpCAM, 5′-AGTTGGTGCACAAAATACTGTCAT-3′, 5′-TCCCAAGTTTTGAGCCATTC-3′, and universal probe #8; CD133, 5′-TCCACAGAAATTTACCTACATTGG-3′, 5′-CAGCAGAGAGCAGATGACCA-3′, and universal probe #83; Bmi1, 5′-TTCTTTGACCAGAACAGATTGG-3′, 5′-GCATCACAGTCATTGCTGCT-3′, and universal probe #63; CD13, 5′-TTGCCTACCAGAACACCATCT-3′, 5′-GTTGGATGGACCGGTTGTT-3′, and universal probe #75; and CD90, 5′-CAGAACGTCACAGTGCTCAGA-3′, 5′-GAGGAGAGAGGGAGAGC-3′, and universal probe #66. To analyze the CD44 splice variants in human HCC cell lines, the following human primer sets (forward and reverse, respectively) were used: CD44, 5′-TCCCAGACGAAGACAGTCCCTGGAT-3′ and 5′-CACTGGGGTGGAATGTGTCTTGGTC-3′, and GAPDH, 5′-AGCCACATCGCTCAGACAC-3′ and 5′-GCCCAATACGACCAAATCC-3′.

Invasion assay

An *in vitro* cell invasion assay was done as previously described (20). Briefly, the invasion rate of tumor cells that migrated through transwell inserts (8-μm pore size) with a uniform layer of BD Matrigel basement membrane matrix (BD Biosciences) was assessed according to the manufacturer's recommended protocol. The cells were seeded (5×10^4) in 500 μL of serum-free medium into the upper chamber of the insert, and medium containing 10% FBS was added to the lower chamber. After 22 hours, the noninvading cells were removed with a cotton swab, and the invading cells were stained with 1% toluidine blue and counted under a microscope.

Patients and treatment

Among the 235 consecutive patients who had undergone curative hepatic resection between 2004 and 2007 in the Department of Gastroenterological Surgery, Graduate School of Medical Sciences, Kumamoto University, 150 primary HCC samples were analyzed in this study. None of the patients received any preoperative anticancer treatment. The pathologic diagnoses and the clinicopathologic

Published OnlineFirst May 2, 2012; DOI:10.1158/0008-5472.CAN-12-0299

factors were established based on the general guideline for primary liver cancer as defined by the Liver Cancer Study Group of Japan (22, 23) and the American Joint Committee on Cancer (AJCC)/International Union Against Cancer (UICC) staging system (24). The median follow-up duration after surgery was 44 months. This study was approved by the Human Ethics Review Committee of the Graduate School of Medicine, Kumamoto University (Kumamoto, Japan).

Immunohistochemistry and scoring

The sample processing and immunohistochemistry (IHC) procedures were carried out as described in a previous report (20). Endogenous peroxidase activity was blocked using 3% hydrogen peroxide, and the sections were incubated with diluted antibodies. A subsequent reaction was carried out with a biotin-free HRP enzyme–labeled polymer from the Envision Plus detection system (Dako Co.). Phospho-Smad2 antibody binding was detected using the Vectastain ABC Elite avidin/biotin/peroxidase kit (Vector Laboratories Inc.). A positive reaction was visualized with the addition of diaminobenzidine solution, which was followed by counterstaining with Mayer's hematoxylin. Primary antibodies for E-cadherin (1:100 dilution; BD), vimentin (1:50 dilution; Santa Cruz), CD44s (1:300 dilution; Bender MedSystems), and phospho-Smad2 (1:100 dilution; Cell Signaling) were used for this study. All of the immunohistochemical staining results were independently scored by 2 pathologists. The membranous E-cadherin, cytoplasmic vimentin, and membranous CD44s expressions were interpreted according to the guidelines published in previous studies (5, 25, 26). For membranous E-cadherin, cytoplasmic vimentin, membranous CD44s, and phospho-Smad2-positive nuclei, we graded the results into categories from 0 to 3+ as follows: 0, no staining; 1+, 1% to 25% staining; 2+, 26% to 50% staining; 3+, >50% of the specimen was stained. For membranous E-cadherin, the 2+ and 3+ samples were defined as positive immunohistochemical results. For cytoplasmic vimentin, membranous CD44s, and phospho-Smad2-positive nuclei, the 3+ specimens were defined as positive immunohistochemical results.

Statistical analyses

All of the experiments were carried out in triplicate, and the data shown are representative of the results. The data are presented as the means ± SD. Independent Student *t* tests were used to compare the continuous variables between the 2

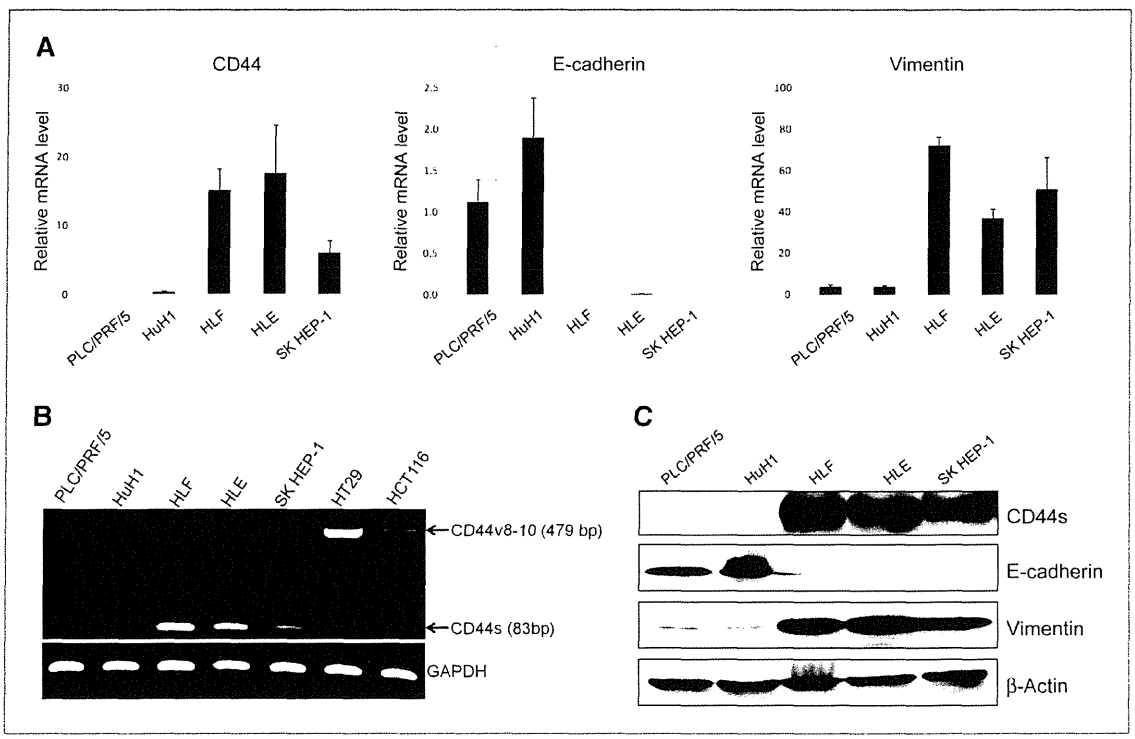

CD44s expression is associated with a mesenchymal phenotype in hepatocellular carcinoma cells. A, the relative expression levels of *CD44*, *E-cadherin*, and *vimentin* mRNA in 5 HCC cell lines are shown. The data represent the means ± SD ($n = 3$). B, RT-PCR analysis of CD44 mRNA in 5 HCC cell lines. Total RNA isolated from the 5 HCC cell lines was subjected to RT-PCR analysis with primers targeted to exons 5 and 16 of human CD44 cDNA and to human GAPDH cDNA. The positions of PCR products derived from CD44v8-10 (479 bp) or CD44s (83 bp) cDNAs are indicated. HT29 and HCT116 cell lines (colon cancer cell lines) were used as positive controls. C, the expression levels of CD44, E-cadherin, and vimentin protein in the 5 HCC cell lines, as determined by Western blot analysis.

Published OnlineFirst May 2, 2012; DOI:10.1158/0008-5472.CAN-12-0299

groups, and categorical variables were compared using the χ^2 test. Overall survival and disease-free survival were calculated using the Kaplan–Meier method and compared using the log-rank test. Statistical analyses were carried out as indicated with a statistical analysis software program (Excel Statistics, Social Survey Research Information Co.). Differences were considered to be significant if $P < 0.05$.

Results

CD44 standard isoform expression is associated with a mesenchymal phenotype in hepatocellular carcinoma cells

We examined the expression of CD44 and its association with EMT markers (E-cadherin and vimentin) in 5 HCC cell lines (PLC/PRF/5, HuH1, HLF, HLE, and SK HEP-1). At the mRNA level, the high CD44 expressing cell lines HLF, HLE, and SK HEP-1 showed high expression levels of vimentin, whereas the low CD44 expressing cell lines PLC/PRF/5 and HuH1 showed high expression levels of E-cadherin, as determined by real-time PCR (Fig. 1A). Recently, we showed that the CD44 isoform expressed in the tumor cells of Gan mice, as well as in human gastrointestinal cell lines, consists mostly of variant isoforms (CD44v8-10) containing amino acids derived from exons 8 to 10 (18, 27). To determine the predominant isoform of CD44 expressed in the HCC cell lines, we examined the expression levels of the different isoforms using RT-PCR according to the same method. Unlike in human colon cancer cell lines, our RT-PCR analysis revealed that CD44s mRNA, rather than CD44v8-10mRNA, was the dominant form present in the human HCC cell lines HLF, HLE, and SK HEP-1 (Fig. 1B). We confirmed the associations of CD44s with E-cadherin and vimentin expression at the protein level (Fig. 1C). These results suggested that high levels of CD44s expression are related to a mesenchymal phenotype, which includes downregulation of E-cadherin and upregulation of vimentin, in HCC cells. We also examined the expression of other CSC markers that were previously reported in HCC (12, 28–31) and compared them with the expression of E-cadherin and vimentin. However, no correlations were observed that were similar to that of CD44 and vimentin. In addition, the expression levels of EpCAM, CD133, and CD13 seemed to be similar to the expression level of E-cadherin (Supplementary Fig. S1).

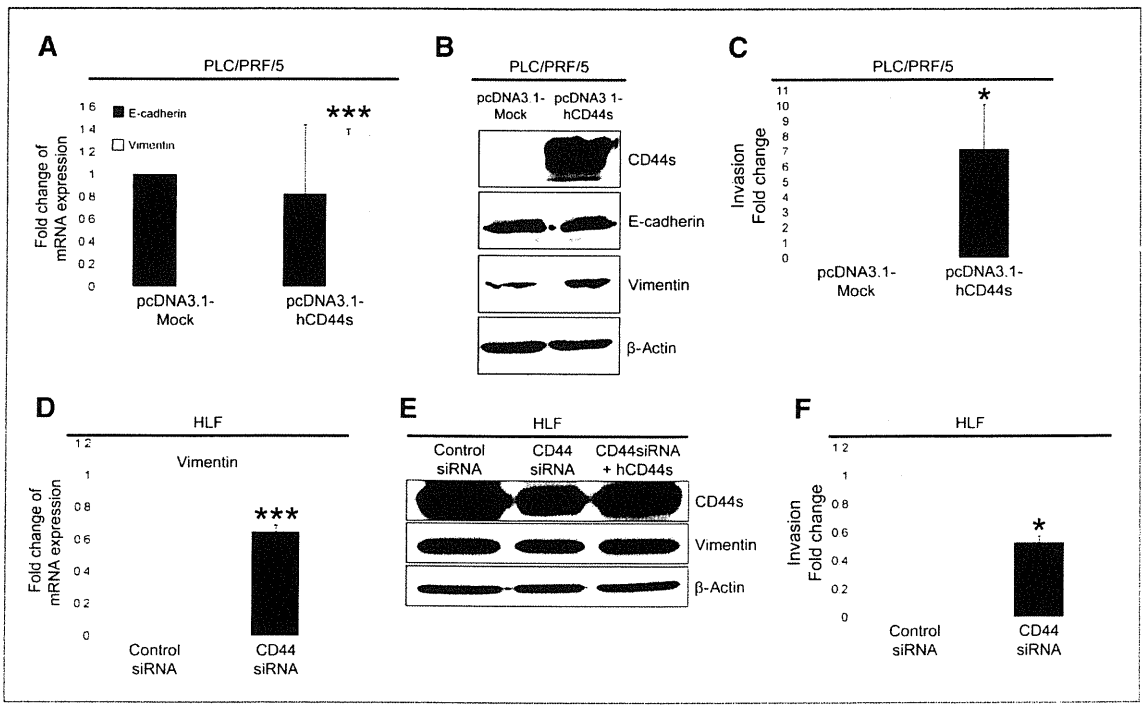

Figure 2. Overexpression of CD44s promotes the expression of vimentin and tumor invasiveness of hepatocellular carcinoma cells whereas the knockdown of CD44s attenuates these changes. A, the relative expression levels of *E-cadherin* and *vimentin* mRNA in PLC/PRF/5 cells overexpressing *CD44s* compared with control cells. The data represent the means ± SD ($n = 3$; ***, $P < 0.001$). B, the expression levels of CD44s, E-cadherin, and vimentin proteins in PLC/PRF/5 cells overexpressing CD44s compared with control cells. C, the invasive capacity of PLC/PRF/5 cells overexpressing CD44s compared with control cells. The data represent the means ± SD ($n = 3$; *, $P < 0.05$). D, the relative expression levels of *vimentin* mRNA in HLF cells transfected with siRNA targeted against CD44 compared with control cells. The data represent the means ± SD ($n = 3$; ***, $P < 0.001$). E, the expression levels of CD44s and vimentin protein in HLF cells transfected with siRNA targeted against CD44 or transfected with both siRNA targeted against CD44 and an hCD44s expression vector compared with control cells. F, the invasive capacity of HLF cells transfected with siRNA targeted against CD44 compared with control cells. The data represent the means ± SD ($n = 3$; *, $P < 0.05$).